Product Traceability and Uncertainty for the NDACC UV-visible spectroscopy total column ozone product

Version 0.6

GAIA-CLIM
Gap Analysis for Integrated
Atmospheric ECV Climate Monitoring
Mar 2015 - Feb 2018

A Horizon 2020 project; Grant agreement: 640276

Date: 22 January 2018

Dissemination level: PU

Work Package 2 - Compiled by Karin Kreher (BKS), François Hendrick (BIRA), Caroline Fayt (BIRA), Christian Hermans (BIRA) and Michel Van Roozendael (BIRA)

Table of Contents

Version history

Version	Principal updates	Owner	Date
0.1 draft	First draft	BKS	29/07/2017
0.2 draft	Second draft	BKS, NPL	29/11/2017
0.3 draft	Third draft	BKS, BIRA	12/12/2017
0.4 draft	Fourth draft	BKS, BIRA	14/12/2017
0.5 draft	Fifth draft	BKS, BIRA	18/12/2017
0.6 draft	Sixth draft	BKS, BIRA, NPL	26/01/2018
1.0	Final issue	BKS, NPL	1/2/2018

1 Product overview

Product name: Total Column Ozone VCD (Vertical Column Density)
Product technique: DOAS (Differential Optical Absorption Spectroscopy)
Product measurand: Ozone in Dobson Units
Product form/range: Total column integrated along a slant column path
Product dataset: NDACC
Site/Sites/Network location:

- Harestua, Norway, 60.2 °N, 10.8 °E, 596 m asl
- Jungfraujoch, Switzerland, 46.55 °N, 7.98 °E, 3580 m asl

Product time period: 2000 - 2014
Data provider: BIRA-IASB
Instrument provider: BIRA-IASB
Product assessor: Francois Hendrick
Assessor contact email: Francois.Hendrick@aeronomie.be

1.1 Guidance notes

For general guidance see the Guide to Uncertainty in Measurement & its Nomenclature, published as part of the GAIA-CLIM project.

This document is a measurement product technical document which should be stand-alone i.e. intelligible in isolation. Reference to external sources (preferably peer-reviewed) and documentation from previous studies is clearly expected and welcomed, but with sufficient explanatory content in the GAIA-CLIM document not to necessitate the reading of all these reference documents to gain a clear understanding of the GAIA-CLIM product and associated uncertainties entered into the Virtual Observatory (VO).

In developing this guidance, we have created a convention for the traceability identifier numbering as shown in Figure 1. The 'main chain' from raw measurand to final product forms the axis of the diagram, with top level identifiers (i.e. 1, 2, 3 etc.). Side branch processes add sub-levels components to the top level identifier (for example, by adding alternate letters & numbers, or 1.3.2 style nomenclature).

The key purpose of this sub-level system is that all the uncertainties from a sub-level are summed in the next level up.

For instance, using Figure 1 contributors 2a1, 2a2 and 2a3 are all assessed as separate components to the overall traceability chain (have a contribution table). The contribution table for (and uncertainty associated with) 2a, should combine all the sub-level uncertainties (and any additional uncertainty intrinsic to step 2a). In turn, the contribution table for contributor 2, should include all uncertainties in its sub-levels.

Therefore, only the top level identifiers (1, 2, 3, etc.) shown in bold in the summary table need be combined to produce the overall product uncertainty. The branches can therefore be considered in isolation, for the more complex traceability chains, with the top level contribution table transferred to the main chain. For instance, Figure 2 & Figure 3 as an example of how the chain can be divided into a number of diagrams for clearer representation.

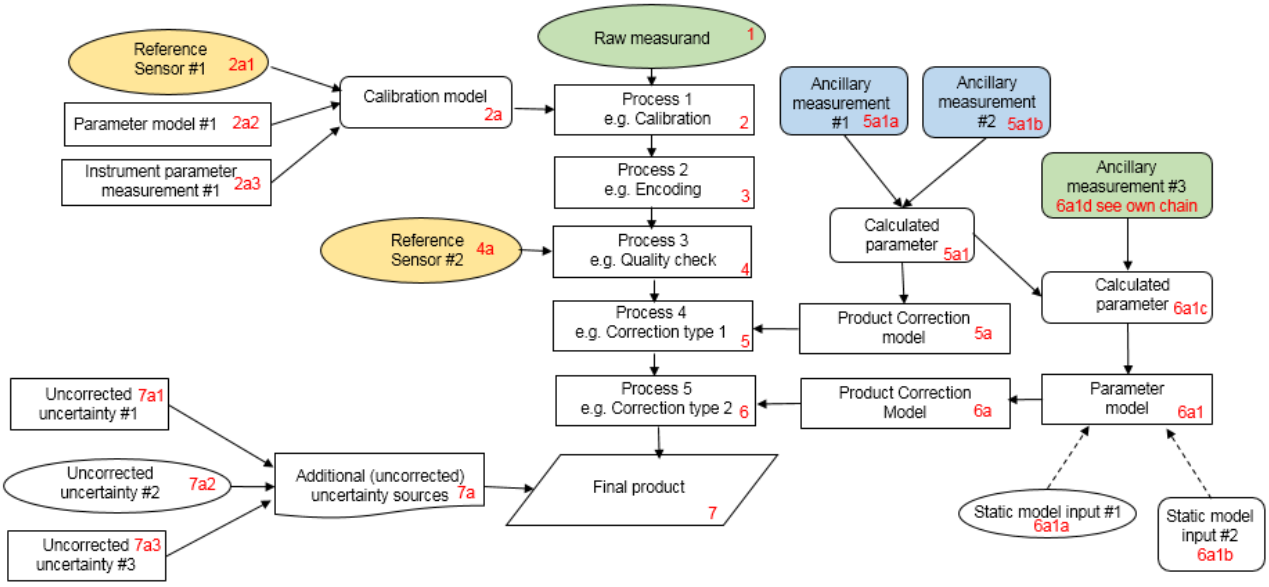

Figure 1. Example traceability chain. Green represents a key measurand or ancillary measurand recorded at the same time with the product raw measurand. Yellow represents a source of traceability. Blue represents a static ancillary measurement

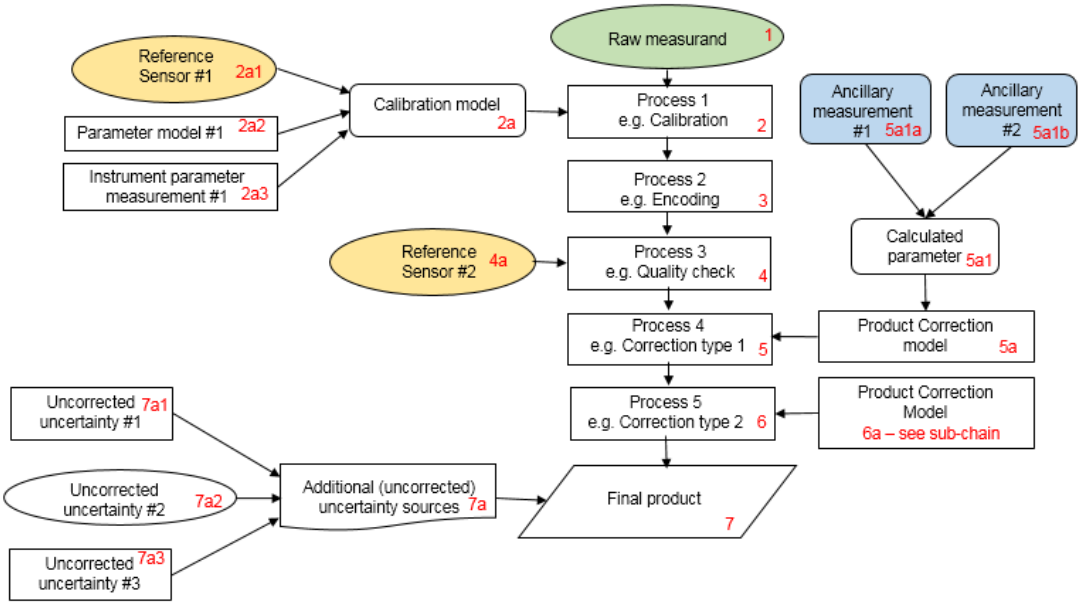

Figure 2. Example chain as sub-divided chain. Green represents a key measurand or ancillary measurand recorded at the same time with the product raw measurand. Yellow represents a source of traceability. Blue represents a static ancillary measurement

When deciding where to create an additional sub-level, the most appropriate points to combine the uncertainties of sub-contributions should be considered, with additional sub-levels used to illustrate where their contributions are currently combined in the described process.

A short note on colour coding. Colour coding can/should be used to aid understanding of the key contributors, but we are not suggesting a rigid framework at this time. In Figure 1, green represents a key measurand or ancillary or complementary measurand recorded at the same time with the raw measurand; yellow represents a primary source of traceability & blue represents a static ancillary measurement (site location, for instance). Any colour coding convention you use, should be clearly described.

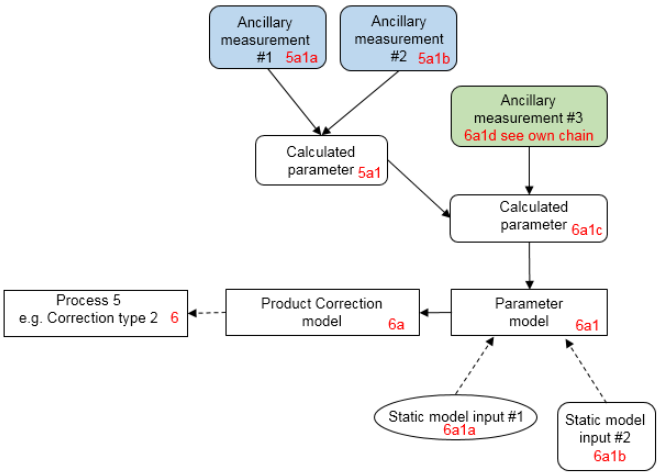

Figure 3. Example chain contribution 6a sub-chain. Green represents a key measurand or ancillary measurand recorded at the same time with the product raw measurand. Blue represents a static ancillary measurement

The contribution table to be filled for each traceability contributor has the form seen in Table 1.

Table 1. The contributor table.

Information / data	Type / value / equation	Notes / description
Name of effect		
Contribution identifier		
Measurement equation parameter(s) subject to effect		
Contribution subject to effect (final product or sub-tree intermediate product)		
Time correlation extent & form		
Other (non-time) correlation extent & form		
Uncertainty PDF shape		
Uncertainty & units		
Sensitivity coefficient		
Correlation(s) between affected parameters		
Element/step common for all sites/users?		
Traceable to …		
Validation		

Name of effect – The name of the contribution. Should be clear, unique and match the description in the traceability diagram.

Contribution identifier - Unique identifier to allow reference in the traceability chains.

Measurement equation parameter(s) subject to effect – The part of the measurement equation influenced by this contribution. Ideally, the equation into which the element contributes.

Contribution subject to effect – The top level measurement contribution affected by this contribution. This can be the main product (if on the main chain), or potentially the root of a side branch contribution. It will depend on how the chain has been sub-divided.

Time correlation extent & form – The form & extent of any correlation this contribution has in time.

Other (non-time) correlation extent & form – The form & extent of any correlation this contribution has in a non-time domain. For example, spatial or spectral.

Uncertainty PDF shape – The probability distribution shape of the contribution, Gaussian/Normal Rectangular, U-shaped, log-normal or other. If the form is not known, a written description is sufficient.

Uncertainty & units – The uncertainty value, including units and confidence interval. This can be a simple equation, but should contain typical values.

Sensitivity coefficient – Coefficient multiplied by the uncertainty when applied to the measurement equation.

Correlation(s) between affected parameters – Any correlation between the parameters affected by this specific contribution. If this element links to the main chain by multiple paths within the traceability chain, it should be described here. For instance, SZA or surface pressure may be used separately in a number of models & correction terms that are applied to the product at different points in the processing. See Figure 1, contribution 5a1, for an example.

Element/step common for all sites/users – Is there any site-to-site/user-to-user variation in the application of this contribution?

Traceable to – Describe any traceability back towards a primary/community reference.

Validation – Any validation activities that have been performed for this element?

The summary table, explanatory notes and referenced material in the traceability chain should occupy <= 1 page for each element entry. Once the summary tables have been completed for the full end-to-end process, the uncertainties can be combined, allowing assessment of the combined uncertainty, relative importance of the contributors and correlation scales both temporally and spatially. The unified form of this technical document should then allow easy comparison of techniques and methods.

2 Introduction

This document presents the Product Traceability and Uncertainty (PTU) information for the NDACC UV-visible spectroscopy total column ozone product, and in particular for the BIRA measurements made at Harestua and Jungfraujoch. The aim of this document is to assess the current status of the traceability and uncertainty information and to provide supporting information for the users of this product within the GAIA-CLIM VO. The uncertainty and traceability information contained in this document is based on the details given in Hendrick et al, 2011 and the NORS report. (http://nors.aeronomie.be/projectdir/PDF/NORS_D4.3_UB.pdf)

The Network for the Detection of Atmospheric Composition Change (NDACC) consists of a set of globally distributed research stations providing consistent, standardized, long-term measurements of atmospheric trace gases, such as ozone. The aim of the network is to 1) detect changes and trends in atmospheric composition and understanding their impact on the stratosphere and troposphere, 2) to establish scientific links and feedbacks between climate change and atmospheric composition, 3) to validate atmospheric measurements from satellites, 4) to support process-focused scientific field campaigns, and to test and improve theoretical models of the atmosphere.

Within NDACC, the UV-vis Working Group includes more than 35 certified UV-visible spectrometers which are deployed worldwide from pole to pole. With an emphasis on the long-term evolution of the ozone layer, these instruments have provided more than two decades of regular measurements of total column amounts of O_3 but also NO_2, BrO and OClO retrieved from zenith scattered sunlight DOAS (Differential Optical Absorption Spectroscopy) observations.

DOAS is a measurement technique used to determine the amount of atmospheric trace gas species, such as ozone, by analysing zenith-sky spectra at large solar zenith angles (SZAs). For the analysis of total column ozone, the absorption features of ozone and other relevant trace gases are fitted in the Chappuis bands within a wavelength window of 450-550 nm using a nonlinear least-squares fitting algorithm. This wavelength range avoids contamination by the strongest water vapour (H_2O) andozygen dimer (O_4) absorption bands while allowing for a good ozone retrieval. Because the light source is the sun and the sun is low on the horizon at large SZA, this allows for a long light path through the atmosphere and the depth of the absorption of the trace gas of interest is used to determine the amount of trace gas measured along the slant paths the sunlight travels through the atmosphere before arriving at the detector. Hence, the product of the spectral analysis are the slant column densities (SCDs), which are then converted into vertical column densities (VCDs) using so-called air mass factors (AMFs) derived by radiative transfer (RT) calculations from locally measured or climatological ozone and air density profiles (see traceability chain in Figure 2 for a more explicit overview).

Hendrick et al. (2011) conclude that the precision in the total column ozone measurements is 4.7% at 1σ level to which the largest contribution is coming from the AMF and from the uncertainty in the SCD estimated to be 3% (1σ) at twilight (including the impact of unknown instrumental and systematic misfit effects) and that the total accuracy, important for comparison with other instruments, is 5.9 %.

3 Instrument description

Although there is quite a variety of individual designs for DOAS instruments (see e.g. Figure 3 in Piters et al. 2012), in general, DOAS instruments consist of: (1) the receiving optics (telescope) to collect the light and guide it into the spectrometer, (2) a grating spectrometer to separate the radiation into the different wavelengths and to re-image them onto a detector, and (3) a detector to convert the spectrum into a signal which is then read out and transferred to the control computer.

At the Jungfraujoch station, the BIRA-IASB SAOZ (Système d'Analyse par Observation Zénithale) instrument has been operated by BIRA-IASB at the Jungfraujoch station from early 1990's to 2014 (see Figure 4, left). It is a broad-band (300-600 nm), medium resolution (~1 nm) diode-array UV-vis spectrometer that measures zenith scattered sunlight (Pommereau and Goutail, 1988). Between 1990 and 2009 two different versions of the SAOZ instrument were used. The first (NMOS) described in Van Roozendael et al. (1994) is based on a Jobin-Yvon spectrometer (model CP200) coupled to a 512 diode Hamamatsu NMOS detector. In December 1998, the system was upgraded to a 1024 diode Hamamatsu detector. This second version (SAM) provides low sun spectra with a better resolution and a higher signal to noise ratio than the NMOS version. The equipment is operated outside, placed in a dust-and-water proof container. The zenith-sky light is collected through a quartz window with a total field of view of 10°. Measurements are performed from sunrise to sunset up to a SZA of 94°.

Since July 2010, a research-grade MAX-DOAS spectrometer has been operated by BIRA-IASB in parallel to the SAOZ instrument, at the Jungfraujoch station (see Figure 4, right). In brief, it is a dual-channel system composed of two grating spectrometers covering the UV (300 – 390 nm) and visible (400 – 580 nm) wavelength ranges and connected to cooled CCD detectors. The instrumental function is close to a Gaussian with a full width at half maximum (FWHM) of 0.4 nm and 0.5 nm in the UV and visible, respectively. The optical head is mounted on a commercial sun tracker (INTRA, Brusag) and is linked to the spectrometers through optical fibres. The instrument is pointing towards the city of Berne (northwest direction) and a full MAX-DOAS scan consists of the following elevation angles: -10°, -8°, -6°, -4°, -2°, 0°, 1°, 3°, 4°, 5°, 8°, 10°, 15°, 30°, and 90° (zenith). For the retrieval of total O_3 columns, only the twilight zenith-sky observations are used.

Figure 4: Pictures of the SAOZ (left) and research-grade MAX-DOAS spectrometers.

The Harestua instrument consists of two commercial grating spectrometers (ORIEL MultiSpec, 12 cm focal length) mounted together outdoor inside a protection case thermally regulated and continuously flushed with dry nitrogen (see Figure 5). Light from the zenith sky is collected through hemispherical quartz domes and directed towards the entrance of each spectrometer using a depolarising quartz-fibre bundle, which also serves as entrance slit (200 micron width). Spectra are

recorded using 1024 pixels cooled diode-array detectors covering respectively the region from 400 to 560 nm with a resolution of 1.2 nm (Spectrometer 1), and the region from 320 to 395 nm with a resolution of 0.7 nm (Spectrometer 2). Two computers (PC) control the acquisition of the spectra. Measurements are performed from sunrise to sunset up to a SZA of 96°. This instrument was continuously operated from January 1998 to April 2013. In November 2012, a new generation instrument based on a similar design was installed to take over from the old one.

Figure 5: Picture of the Harestua instrument currently in operation.

4 Total O_3 column algorithm

Total O_3 VCDs are retrieved from twilight zenith-sky UV-visible spectroscopy observations using the standard NDACC approach described in Hendrick et al., 2011 (see also http://ndacc-uvvis-wg.aeronomie.be/tools.php). This method is based on the following expression:

$$VCD(\theta) = \frac{DSCD(\theta) + RCD}{AMF(\theta)} \quad (1)$$

where VCD(θ) is the O_3 VCD at solar zenith angle (SZA) θ, DSCD(θ) is the O_3 differential slant column density (DSCD) at SZA θ, RCD is the residual O_3 amount in the reference measurement (a fixed spectrum usually recorded at high sun around local noon), and AMF(θ) the so-called air mass factor at SZA θ.

First, zenith radiance spectra are analyzed using the DOAS (Differential Optical Absorption Spectroscopy) technique (Platt and Stutz, 2008). The O_3 DSCD, which is the primary product of the DOAS analysis, is retrieved in the 450-550 nm wavelength range, taking into account the spectral signatures of NO_2, H_2O, O_4, and the filling-in of the solar Fraunhofer bands by the Ring effect (Grainger and Ring, 1962). The O_3 absorption cross-sections at 223 K are from Bogumil et al. (2003).

A third- to fifth-order polynomial is used to fit the low frequency spectral structure due to molecular and Mie scattering.

In a second step, the absolute O_3 SCD at SZA θ is calculated by adding the RCD to the DSCD(θ), the RCD being determined using the Langley plot method based on Vaughan et al. (1997). The VCD(θ) is then derived by dividing the absolute O_3 SCD at SZA θ by an appropriate AMF(θ). For the selection of the SZA range representative of twilight conditions, the best compromise between accuracy and precision is achieved in the 86-91° SZA range. The recommended approach is to apply a linear fit on VCDs in the above SZA range and then derive the column value at an effective SZA, which is usually fixed at 90°.

The standard O_3 AMF climatology used in the NDACC total O_3 retrieval is based on the TOMS version 8 (TV8) ozone and temperature profile climatology (Bhartia et al., 2004). It consists of 18 LUTs generated using the UVSPEC/DISORT RTM initialised with TV8, each of these LUT corresponding to one TV8 latitude (10° latitude bands between 90°S and 90°N) (Hendrick et al., 2011). The other entry parameters are: wavelength, ground albedo, altitude of the station, day of the year, and SZA. The extraction of appropriate O_3 AMFs for a given station is done by using the dedicated interpolation routine developed in the framework of the NDACC UV-vis WG (see http://ndacc-uvvis-wg.aeronomie.be/tools.php).

5 Product Traceability Chain

The product traceability chain (Figures 6a and 6b) describes each processing step from the raw data (raw radiance spectra) via an intermediate product (differential slant column density - DSCDs) to the final product (quality-controlled total ozone vertical column density - VCD). This chain includes all the calibration and quality control procedures applied within the processing routine.

The complete traceability chain has been divided in 2 parts to be more legible with Figure 6a displaying the first part of the processing chain up to the DSCDs which also includes the physical chain. Elements (A) – (E) in Figure 6a display the steps of the physical chain with solar radiation (A) as input and symbols (B) – (D) representing the main instrumental parts of the DOAS instrument culminating into the measurand which is the raw radiance spectrum (E) and the starting point for the processing chain. As already described under Section 3, the DOAS instruments considered here have two separate units, one containing the telescope and calibration unit (B), and the other one consisting of spectrometer, detector and computer, discussed further under (C) and (D).

(B) Entrance optics

The entrance optics consists of a telescope and a fibre bundle which feeds the light into the spectrometer. This set-up has several advantages:

1 As fibre bundles have low light losses, they can be quite long (many meters), resulting in flexible set-up options.
2 If the individual fibres within a bundle have a small enough diameter, a fibre bundle can be configured to have a circular aperture at the telescope side and a rectangular shape at the spectrometer slit. This reduces light losses at the slit side of the fibre and minimises the field-of-view of the instrument for the same throughput at the other side, since the later depends on the fibre bundle total diameter.
3 If long enough, quartz fibres are depolarising, minimizing effects from the polarisation dependency of most grating spectrometers in combination with the polarised nature of Rayleigh scattered light.

4 If long enough, quartz fibres cause mode mixing leading to a more homogenous illumination of the spectrometer. Mode mixing can be enhanced by using additional treatment of the fibres, e.g. by increasing the bending angles of the fibres.

Any instrumental effects arising from the type of entrance optics used will be dealt with in the processing chain with element identifiers 3, 4 and 5 (including the respective sub-chains).

(C) Grating Spectrometer

The most important parameters for characterising the spectral properties of a DOAS instrument are its spectral range, the spectral resolution, the spectral sampling and the stability of the spectral recording. The spectral range needs to be large enough to cover the spectral window of interest, and it is usually advisable to have a slightly wider range than actually needed to avoid having to use the edge of the detector. The required spectral resolution depends on species and is usually between 0.2 and 1.0 nm. In general, better spectral resolution improves the information content of the measurements but it also reduces the overall throughput and thus the signal to noise ratio. The optimum choice therefore depends on instrument and species. Spectral sampling needs to be large enough to allow good interpolation of the spectra. Spectral stability is vital for good DOAS fits and one should aim at having stability better than at least $1/10^{th}$ of a detector pixel by temperature stabilising the spectrometer.

Spectrometer straylight can be an issue for measurements particularly in the UV as it decreases apparent absorptions of atmospheric trace gases. Spectral straylight (photons detected in the incorrect spectrometer wavelength channel) is present in all instruments. Accurate characterisation of straylight is best performed with a powerful monochromatic light source (tunable laser) operated at different wavelengths. Alternatively, for a more qualitative analysis, optical cut-off filters can be applied which are opaque for wavelengths below a certain threshold in combination with a broadband or monochromatic light source. However, in DOAS analyses usually a measured spectrum is analysed against a Fraunhofer reference spectrum, which is typically affected by a similar straylight level, often the fitted additional offset is found to be small, while the actual straylight level of the individual spectra might be much larger.

Polarisation sensitivity: The efficiency of both gratings and mirrors is polarisation dependent, and therefore most spectrometers used in DOAS instruments have pronounced polarisation dependency. As atmospheric light is polarised by both Rayleigh and aerosol scattering effects, with their magnitude depending on the relative position of sun and viewing direction, this can create problems in the data analysis. Therefore, most instruments employ fibre optics which are depolarising which is also the case for the instruments discussed here (see also discussion of entrance optics above).

Slit function or instrument transfer function describes the response of the instrument to a monochromatic input. As a result of a finite slit width, spectrometer resolving power and aberrations, and detector pixel size, even a single wavelength input will result in a broadened and blurred line on the detector. Section 6.5 describes in more detail how the slit function is characterised and used within the data processing.

These effects are all dealt with as part of the data processing and are covered in the processing chain under element identifiers 3, 4 and 5 (including the respective sub-chains).

(D) Detector (CCD, PDA)

Several sources contribute to the spectral or instrumental noise. These include photon noise, readout noise and dark current noise. Instrumental noise can be determined by calculating the root mean

square of the ratio of two subsequent spectra from a smooth light source (e.g., a halogen lamp). Since the observed signal follows Poisson statistics, the noise level should decrease with the square root of the signal. It is recommended to determine the noise level by calculating the ratio of many spectra at short integration time using a constant light source. A log-log plot of the resulting noise as a function of number of added spectra should yield a straight line with a slope of -0.5. Deviations from this behaviour are an indicator for additional noise sources other than photon noise.

Dark signal is composed of two components – an electronic offset which is artificially added to the signal independent of exposure time and a second term which increases with exposure time. Both terms depend on temperature and can therefore change during operations. Two different approaches can be used to characterise the dark signal: Either, only a limited set of exposure times is used during measurements and dark measurements for each of these exposure times are then subtracted during data calibration. Alternatively, the two components of the dark signal can be determined independently of each other by using very short exposure times for the offset and one or several long exposure times for the dark current. The latter approach allows computation of the dark signal for arbitrary exposure times and is used for the instruments and data analysis discussed here. To characterise changes of dark signal over time, dark measurements should be repeated on a regular basis. The dark signal and its treatment is further discussed under section 6.2

Detector linearity: Good linearity of the detector is a prerequisite for accurate DOAS retrievals as otherwise the large dynamic range of individual spectra introduced by the Fraunhofer lines would result in artefacts at the positions of Fraunhofer lines. Often, detectors deviate from strictly linear behaviour at very low and very large signals, with decreasing efficiency when nearing saturation. For instruments having detectors with non-linear behaviour, the range of good linearity should be determined in the lab and the exposure times during measurements should be selected to result in signals within the linear range. Deviations from linearity can also be characterised and corrected to some degree on the measurements. Nonlinearities can originate from the pixels of the detector or from the electronics processing the signal of the detector and are therefore either pixel specific or common to all pixels. In most instruments, the latter effect dominates.

Detector pixel-to-pixel variability: Both CCD and Photo Diode Array (PDA) detectors have small variations in sensitivity from pixel to pixel. This will cancel when taking the ratio between two measurements taken with the same instrument, but only if the spectral calibration is completely stable. If this is not the case, pixel-to-pixel variability will introduce high frequency structures in the residuals.
Pixel-to-pixel variability can be characterised by taking a measurement with a broadband light source and applying a high pass filter on the result, for example by subtracting a version of the image / spectrum which has been smoothed over 5 pixels. Dividing all measurements pixel wise by this correction will cancel most of the detector variability. As pixel-to-pixel variability is a detector property which usually does not change over time, it is sufficient to characterize it once.

Temperature dependence: Temperature changes of the instrument can influence the operation of instrument in several ways. In particular, for instruments not having a temperature stabilisation, the spectral calibration of the instrument (conversion of pixel number to wavelength) will change with temperature as result of mechanical changes of the instrument. This necessitates application of shift and stretch spectral corrections in the DOAS analysis. In addition, defocusing due to mechanical changes can lead to changes in slit function which impact on the residual and the absolute accuracy of the absorption measurements. This can be at least partly compensated by fitting the slit function in the DOAS retrieval but is limited by parametrisation of the shape of the slit function and computation time. Characterisation of the temperature dependence of the instrument can be done by systematically changing the instrument temperature by heaters or coolers over a temperature range covering all expected instrument temperatures while taking measurements of a spectral line lamp.

These effects are all dealt with as part of the data processing and are covered in the processing chain under element identifiers 2 and 5 (including the respective sub-chains).

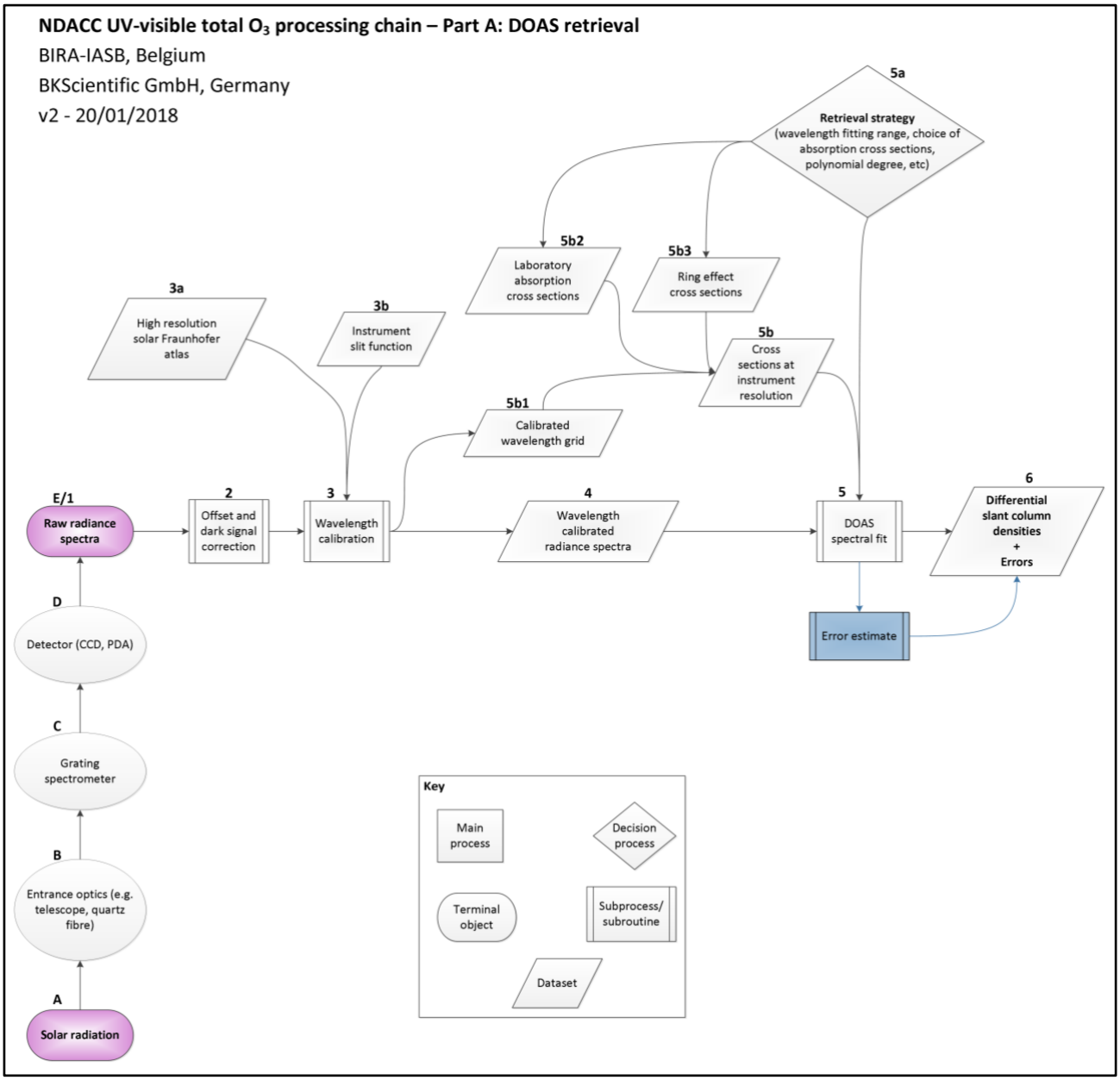

Figure 6a: Traceability chain for UV-visible spectroscopic measurements of total column O_3. The first part shows the chain from the initial raw radiance spectra (1) to the differential slant column densities (6) including all side chain elements. The key lists all the shapes used within the processing chain. This diagram also shows the physical chain (A) – (E) with the oval shape marking important instrumental parts.

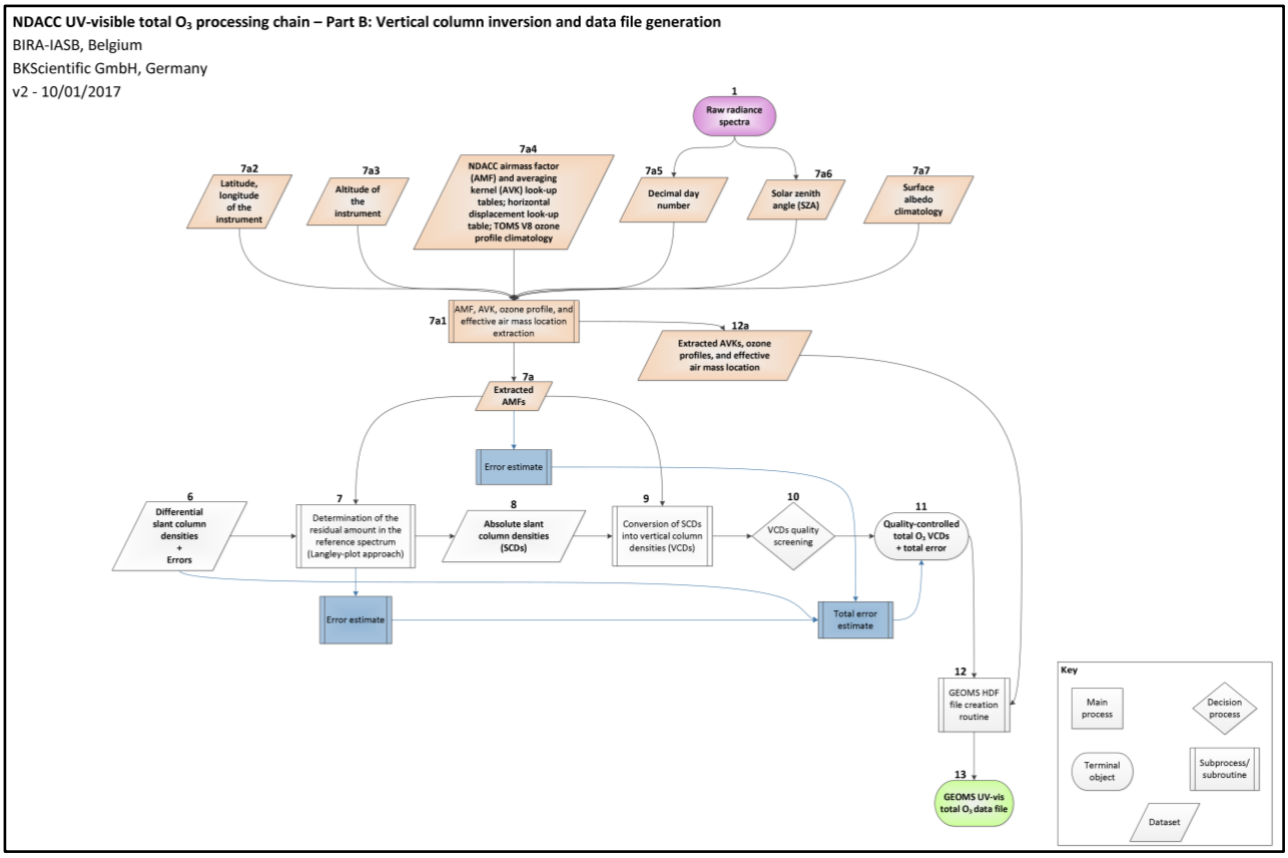

Figure 6b: Traceability chain for UV-visible spectroscopic measurements of total column O_3. The second part shows the chain from the differential slant column densities (6) to the final UV-vis total column ozone data product (13) including all side chain elements.

6 Element contributions

6.1 Raw radiance spectra (1)

As described in more detail in Section 3, the MAX-DOAS instrument at Jungfraujoch is making MAX-DOAS measurements (as in acquiring raw radiance spectra) during most of the day but is looking up in the zenith during twilight. For the retrieval of total O_3 columns, only these twilight zenith-sky observations (86-91° SZA) are used. The same is also true for the measurements made at Harestua. At both stations, the integration time is about 2 minutes around 90° SZA and this corresponds to the accumulation of one single scan.

Photon noise results from the inherent statistical variation in the arrival rate of photons incident on the CCD or PDA. Photoelectrons generated within the semiconductor device constitute the signal, the magnitude of which fluctuates randomly with photon incidence at each measuring location (pixel) on the CCD. The interval between photon arrivals is governed by Poisson statistics, and therefore, the photon noise is equivalent to the square-root of the signal.

Information / data	Type / value / equation	Notes / description
Name of effect	Raw radiance spectra	Light intensity measured in counts per pixel/diode
Contribution identifier	(1)	
Measurement equation parameter(s) subject to effect	$L_{raw} = L_{raw}$	No measurement equation, the uncertainty considered here is photon noise, other contributions are considered further down the chain
Contribution subject to effect (final product or sub-tree intermediate product)	Wavelength calibrated radiance spectra	
Time correlation extent & form	None	
Other (non-time) correlation extent & form	None	
Uncertainty PDF shape	Normal	
Uncertainty & units	$Lraw_{noise} = \sqrt{signal}$ Photon noise in photoelectron S/N ratio typically between 1000 and 10000	Square-root of the signal in photoelectrons. Photon noise can be easily estimated by ratioing spectra acquired under same illumination. DOAS systems typically achieve S/N ratios of a few thousands
Sensitivity coefficient	1	
Correlation(s) between affected parameters	None	
Element/step common for all sites/users?	Yes	
Traceable to …	N/A	statistical
Validation	N/A	

6.2 Offset and dark signal correction (2)

All raw radiance spectra are corrected for their **offset and dark current contribution** (for more details, see Section 5).

Brief description of dark current & offset: The electronic offset is artificially added to the signal independent of exposure time while the dark current increases with exposure time. As both, the dark signal and electronic offset, depend on temperature, it is useful to stabilise the temperature of the CCD or PDA and associated electronic parts to ±1 K or preferably better accuracy even if it is not cooled.

The BIRA spectrometers at Harestua and Jungfraujoch are kept around 235 K by means of a thermoelectric Pelletier cooling system (accuracy: ±0.1 K (1σ)). In addition, the whole setup, excluding the CCD, is mounted inside a box thermally regulated using a second Pelletier system (accuracy: ±1 K (1σ)). In order to minimize thermal stress on mechanical and optical parts. The correction of daytime spectra for dark current is performed using night time dark current measurements (filter wheel in close position).

Information / data	Type / value / equation	Notes / description
Name of effect	Offset and dark current correction	Platt & Stutz, 2008
Contribution identifier	(2)	
Measurement equation parameter(s) subject to effect	$L_{offset\_cor} = L_{raw} - (L_{dc} + L_{offset})$	
Contribution subject to effect (final product or sub-tree intermediate product)	Wavelength calibrated radiance spectra	
Time correlation extent & form	24 hours	In the case of Harestua and Jungfraujoch instruments, dark current is measured every night using the filter wheel in the close position. A time correlation is therefore not expected.
Other (non-time) correlation extent & form	None	
Uncertainty PDF shape	Normal	The uncertainty in the offset and dark current correction is very small; night to night differences minimal
Uncertainty & units (1σ)	Square-root of number of thermal electrons per second $Noise_{dark} = \sqrt{dark\ signal}$ Around 0.1%	Dark current level is typically around 600cts out of 30000cts; The uncertainty on the combined dark current + offset is around 25cts
Sensitivity coefficient	1	
Correlation(s) between affected parameters	None	
Element/step common for all sites/users?	Yes	
Traceable to …	Community agreed procedure	
Validation	N/A	

6.3 Wavelength calibration (3)

The **wavelength calibration** (e.g. see Platt and Stutz, 2008) of the reference spectrum is firstly determined using a lamp spectrum (e.g. Hg calibration lamp) and secondly, and more importantly, using a procedure based on the alignment of the Fraunhofer structures of the reference spectrum (I_o) with those of an accurately calibrated high-resolution solar reference atlas, degraded to the resolution of the instrument, i.e. convolved with the instrumental slit function (3b). The solar Fraunhofer atlas used for this purpose is the Chance and Kurucz (2010) spectrum.

For the Jungfraujoch and Harestua data sets, calibration lamp spectra are measured once a year. The Fraunhofer calibration is performed for each spectrum as part of the data analysis.

Information / data	Type / value / equation	Notes / description
Name of effect	Wavelength calibration	2 step process: 1. lamp measurement with distinct lines (e.g. Hg) for wavelength calibration, 2. Fraunhofer ref spectrum
Contribution identifier	(3)	
Measurement equation parameter(s) subject to effect	DSCD(θ)	Shift and stretch applied in each analysis sub-regions, to correct the wavelength alignment
Contribution subject to effect (final product or sub-tree intermediate product)	Wavelength calibrated radiance spectra	
Time correlation extent & form	lamp calibration annually, Fraunhofer – spectrum interval.	
Other (non-time) correlation extent & form	None	
Uncertainty PDF shape	Normal	
Uncertainty & units (1σ)	<0.1 nm (1σ)	Note that any residual shift uncertainty, however, is dealt with in the DOAS fit
Sensitivity coefficient	Non-linear	Any shift residual is re-accessed in the DOAS fit.
Correlation(s) between affected parameters	None	
Element/step common for all sites/users?	Yes	
Traceable to …	NIST Atomic Spectra Database (ver 5.5.2), 2018 & Fraunhofer lines traceable to Chance and Kurucz (2010)	
Validation	Sensitivity tests	

6.4 High resolution solar Fraunhofer atlas (3a)

The high resolution solar Fraunhofer atlas spectrum used here within the analysis is the Chance and Kurucz spectrum (2010).

Information / data	Type / value / equation	Notes / description
Name of effect	High resolution solar Fraunhofer atlas	Chance and Kurucz (2010)
Contribution identifier	(3a)	
Measurement equation parameter(s) subject to effect	DSCD(θ)	
Contribution subject to effect (final product or sub-tree intermediate product)	Wavelength calibrated radiance spectra	
Time correlation extent & form	Systematic - one list used for full data record.	
Other (non-time) correlation extent & form	None	
Uncertainty PDF shape	Normal	
Uncertainty & units (1σ)	3.5% – 4% (1σ)	Absolute accuracy of 3.5–4% over the relevant wavelength range addressed. The absolute vacuum wavelength accuracy is <=3.2x10^{4} nm above 305 nm. Chance and Kurucz (2010)
Sensitivity coefficient	1 to wavelength – co-efficient product of DOAS fit.	
Correlation(s) between affected parameters	Wavelength calibration.	
Element/step common for all sites/users?	Yes	
Traceable to …	Traceable back to the wavelength calibration using Chance and Kurucz (2010).	
Validation	N/A	

6.5 Instrument slit function (3b)

The **instrument slit function** or instrument transfer function describes the response of the instrument to a monochromatic input. As a result of a finite slit width, spectrometer resolution

and aberrations and detector pixel size, a single monochromatic wavelength input will result in a broadened and blurred line on the detector. As the solar spectrum is highly structured by Fraunhofer lines, accurate knowledge of the instrument function is important for passive DOAS retrievals to correct for filling-in of Fraunhofer lines by inelastic scattering (Ring effect) (Grainger and Ring, 1962). The instrument slit function is essential to convolute the absorption cross-sections of atmospheric gases. Depending on the instrument type, the slit function can be wavelength dependent. In many instruments it also depends on the temperature of the spectrometer and may change over time.

Therefore, slit function characterisation is a task that needs to be repeated regularly in order to identify and characterize changes in the instrument. Instrumental slit functions are generally characterized in the lab using a spectral line lamp (e.g. HgCd). Temporal changes of the slit function are monitored by taking regular measurements with a spectral line lamp placed in front of the telescope or fiber. For a good representation of the slit function, a full and homogenous illumination of the instrument needs to be ensured (e.g. by using a diffusor). To minimize spectrometer non-linearity effects on the slit function spectra, the emission peaks which are used for the analysis are recorded at a similar saturation as the MAX-DOAS measurement spectra.

A good knowledge of the instrumental slit function and its potential wavelength variation is important to avoid systematic errors in the retrieved slant columns due to spectral shape mismatch between the reference and atmospheric spectra.

In the case of the BIRA spectrometers at Harestua and Jungfraujoch, the corresponding instrument slit functions are characterized using HgCd lamp measurements at the time of installation and maintenance of the systems. In addition, slit functions are automatically adjusted using the DOAS spectral fitting software QDOAS making use of the solar Fraunhofer lines.

Information / data	Type / value / equation	Notes / description
Name of effect	Instrument slit function	
Contribution identifier	(3b)	
Measurement equation parameter(s) subject to effect	$y^*(\lambda) = \int_{-\infty}^{\infty} F(\lambda')y(\lambda - \lambda')d\lambda'$	The instrument slit function is firstly applied to the solar reference spectrum - and further down the chain, secondly to the high-res absorption cross-sections
Contribution subject to effect (final product or sub-tree intermediate product)	Wavelength calibrated radiance spectra	
Time correlation extent & form	Yearly	Annual calibration
Other (non-time) correlation extent & form	None	Instrument temperature is stabilised, if any, just very small temperature fluctuations. Slit width has a thermal dependence,

		however, if this causes changes in the slit width, this will be taken care of in DOAS analysis accordingly, as the line width is a DOAS fit variable.
Uncertainty PDF shape	Normal	
Uncertainty & units (1σ)	<0.1%	The uncertainty on the broad Chappuis ozone cross-section due to ISRF errors is very small (<0.1%), however the error on fitted ozone SCD due to possible misfits introduce by ISRF errors on the Ring effect, or water vapour absorption at 510 nm is larger and can possibly reach the percent level.
Sensitivity coefficient	1	
Correlation(s) between affected parameters	None	
Element/step common for all sites/users?	Yes	
Traceable to …	The slit function is generally recorded in an ASCII file associated to the spectra files.	Community agreed procedure
Validation	Intercomparisons campaigns	e.g. Piters et al., 2012; Roscoe et al, 2010, Vandaele et al., 2005

6.6 Wavelength calibrated radiance spectra (4)

Given the importance of the wavelength registration for DOAS evaluations in general, the measured spectra have to be aligned with the highest accuracy. This is achieved by correlating the measured spectra with an accurately calibrated high-resolution solar reference spectrum (Chance and Kurucz, 2010) degraded to the resolution of the instrument, i.e. convolved with the instrumental slit function. Least-squares techniques as implemented in the QDOAS software suite (http://uv-vis.aeronomie.be/software/QDOAS/QDOAS_manual.pdf) are used to align the spectra accurately with the Fraunhofer reference.

Wavelength scale shift and stretch are taken into account in the wavelength calibration scheme. To this end, the spectral interval is divided into a number of equally spaced sub-intervals. The fitting algorithm used for the DOAS retrieval is then applied in each sub-interval to fit the measured intensities to those of the high-resolution solar spectrum, according to the equation

$$I_0(\lambda) = I_S(\lambda - \Delta_i)\exp(-\sum_{j=1}^{m} S^j c_j)$$

where I_S is the solar spectrum convolved at the resolution of the instrument assuming symmetric (Harestua) or asymmetric (Jungfraujoch) Gaussian line shapes, Δ_i is a fitted constant shift in sub-interval i, and the c_j are optional absorber coefficients accounting for possible light absorption in the reference spectrum I_0. A value of the shift Δ_i is calculated in each sub-interval i and a polynomial is fitted through the individual points in order to reconstruct an accurate wavelength calibration $\Delta(\lambda)$ for the complete analysis interval.

Information / data	Type / value / equation	Notes / description
Name of effect	Wavelength calibrated radiance spectra	This is a product, not a processing step
Contribution identifier	(4)	
Measurement equation parameter(s) subject to effect	$I_0(\lambda) = I_S(\lambda - \Delta_i)\exp(-\sum_{j=1}^{m} S^j c_j)$	
Contribution subject to effect (final product or sub-tree intermediate product)	Differential slant column of ozone	
Time correlation extent & form	None	
Other (non-time) correlation extent & form	None	
Uncertainty PDF shape	Normal	Assumed
Uncertainty & units (1σ)	Uncertainty in wavelength shift in nm, same as in (3) but not to be added up into the summary	
Sensitivity coefficient	1	For small shift values, DSCD errors will scale linearly with shift errors. This can easily be shown by linearizing shift and stretch terms in the DOAS equation.
Correlation(s) between affected parameters	None	
Element/step common for all sites/users?	Yes, but actual numbers are instrument specific	
Traceable to …	Fraunhofer lines traceable back to the wavelength calibration using Chance and Kurucz (2010).	
Validation	N/A	

6.7 DOAS spectral fit (5)

Each “to-be-analysed” spectrum is ratioed with a so-called “reference” spectrum to remove the

dominating Fraunhofer bands and, if relevant, some instrumental artefacts. This "ratio" spectrum is then fitted with the absorption convolved cross-sections of the absorbers relevant for the wavelength range chosen for the analysis. Before the ratio is taken, as part of the fitting procedure, it is essential to properly align the analysed spectrum with respect to the reference using shift and stretch, before taking the ratio. This optimisation is performed as part of the DOAS retrieval procedure using a non-linear iterative least-squares scheme (Marquardt-Levenberg).

For total column retrievals of O_3 from zenith-sky UV-visible spectra the recommended wavelength range is 450-550 nm and absorption cross-sections for O_3, NO_2, H_2O and O_4 are used as well as a Ring cross-section to correct for the filling in of the Fraunhofer bands (Ring effect), a polynomial term to filter out broadband atmospheric attenuation and an offset term to deal with straylight in the spectrometer.

Errors associated to the least-squares fit are due to detector noise, instrumental imperfections (small wavelength scale and resolution changes, etaloning and non-linearities of the detector, stray-light, polarisation effects, etc.) as well as errors or unknowns in the signal modelling (Ring effect, unknown
absorbers, wavelength dependence of the AMF, etc). To some extent, such errors are pseudo-random in nature and, as such, can be estimated statistically from the least-squares fitting procedure. Fitting errors derived from the least-squares analysis typically give uncertainties of the order 5 DU for O_3 DSCDs around 90° SZA.

Information / data	Type / value / equation	Notes / description
Name of effect	DOAS spectral fit	Adjustable variables within the fitting procedure are: shift and stretch, resolution, absorber concentrations. Aim is to minimise residuals; User judgement involved when fine-tuning the analysis procedure, i.e. we are looking for a residual below a certain threshold
Contribution identifier	(5)	
Measurement equation parameter(s) subject to effect	Differential slant column of ozone	
Contribution subject to effect (final product or sub-tree intermediate product)	Quality controlled total column O_3 VCD	
Time correlation extent & form	Variable – mainly systematic from assumptions & calibration cycle	
Other (non-time) correlation extent & form	None	
Uncertainty PDF shape	normal	
Uncertainty & units (1σ)	13.45×10^{19} molec./cm^2 (5 Dobson unit)	This is the typical uncertainty in slant column

		densities resulting from all effects already combined
Sensitivity coefficient	1	
Correlation(s) between affected parameters	None	
Element/step common for all sites/users?	Yes	
Traceable to …	Community agreed procedure	e.g. Hendrick et al. (2011)
Validation	Intercomparison campaigns	e.g. Piters et al., 2012; Roscoe et al, 2010, Vandaele et al., 2005

6.8 Retrieval strategy (5a)

This step combines all selected constraints and choices for the fitting routine such as wavelength fitting range, choice of absorption cross-sections, polynomial degree, etc. The following settings have been used for the total column O_3 retrieval:

- Fitting interval: 450–550 nm
- Wavelength calibration: based on reference solar atlas (Chance and Kurucz, 2010)
- Cross-sections:
  - O_3 Bogumil et al. (2003), 223° K
  - NO_2 Vandaele et al. (1997), 220° K
  - H_2O Hitran 2010 (Rothman et al., 2010)
  - O_4 Hermans (http://spectrolab.aeronomie.be/o2.htm)
  - Ring effect Chance and Spurr (1997)
- Molecular and aerosol scattering: Polynomial of order 3, or equivalent non-polynomial high-pass filtering
- Determination of the residual amount in the reference spectrum: Langley-plot approach.
- SZA range: 86-91°SZA; the VCD is derived using a linear fit of VCD versus SZA in this range and taking the corresponding value at 90°SZA.

This is a decision making process and hence not associated with its own uncertainties.

Information / data	Type / value / equation	Notes / description
Name of effect	Retrieval strategy	Hendrick et al. (2011); http://ndacc-uvvis-wg.aeronomie.be/tools/NDACC_UVVIS-WG_O3settings_v2.pdf
Contribution identifier	(5a)	
Measurement equation parameter(s) subject to effect	Differential slant column of ozone	
Contribution subject to	Quality controlled total	

effect (final product or sub-tree intermediate product)	column O_3 VCD	
Time correlation extent & form	None	
Other (non-time) correlation extent & form	None	
Uncertainty PDF shape	N/A	
Uncertainty & units (1σ)	N/A	
Sensitivity coefficient	1	
Correlation(s) between affected parameters	N/A	
Element/step common for all sites/users?	N/A	
Traceable to …	N/A	
Validation	Intercomparison campaigns	e.g. Piters et al., 2012; Roscoe et al, 2010, Vandaele et al., 2005

6.9 Cross-sections at instrument resolution (5b)

To account for the generally lower resolution of the spectrometer used for the actual measurements as compared to high-resolution literature cross-sections, the absorption cross-sections listed above in Section 6.8 are convolved with the instrumental slit function (3b) described in Section 6.5 and interpolated on the I_o wavelength grid. Cross-sections can be pre-convolved and interpolated on an appropriate wavelength grid prior to the analysis. However, the direct use of high-resolution cross-sections which can be convolved in real-time with a predefined slit function or with the slit function determined by the wavelength calibration procedure, is more flexible and allows to account for a possible day-to-day variability in the slit function. This latter approach is the baseline used for retrievals in Harestua and Jungfraujoch.

Information / data	Type / value / equation	Notes / description
Name of effect	Cross-sections at instrument resolution	http://ndacc-uvvis-wg.aeronomie.be/tools.php
Contribution identifier	(5b)	
Measurement equation parameter(s) subject to effect	$y^*(\lambda) = \int_{-\infty}^{\infty} F(\lambda')y(\lambda - \lambda')d\lambda'$	Equation used for folding high-res absorption cross-section y with instrument slit function F to get the same spectral resolution as the measurements
Contribution subject to effect (final product or sub-tree intermediate product)	Differential slant column of ozone	

Time correlation extent & form	Possible, e.g. if the XSs are only convolved once but the slit function changes with time	Any such time correlation is strongly minimized owing to the instrumental design, which includes active stabilisation of spectrometers and detectors. In addition, possible fluctuations at the scale of days will be efficiently compensated by the dynamical slit function adjustment performed as part of the wavelength calibration procedure.
Other (non-time) correlation extent & form	None	
Uncertainty PDF shape	Normal	
Uncertainty & units (1σ)	<0.1%	The uncertainty due to the ozone cross-section convolution process is small (<0.1%) and related to the uncertainty on the determination of the slit function.
Sensitivity coefficient	1	
Correlation(s) between affected parameters	None	
Element/step common for all sites/users?	Yes	
Traceable to …	N/A	
Validation	Intercomparison campaigns	e.g. Piters et al., 2012; Roscoe et al, 2010, Vandaele et al., 2005

6.10 **Calibrated wavelength grid (5b1)**

The wavelength grid used here is the wavelength grid of the reference spectrum *Io*, calibrated with respect to the high resolution solar Fraunhofer spectrum. Shift and stretch is taken into account in the wavelength calibration scheme. To this end, the spectral interval is divided into a number of equally spaced sub-intervals. The fitting algorithm used for the DOAS retrieval (QDOAS) is then applied in each sub-interval to fit the measured intensities to those of the high-resolution solar spectrum.

Information / data	Type / value / equation	Notes / description
Name of effect	Calibrated wavelengths	Shift and stretch applied in

	grid	equally spaced sub-intervals determine by the user
Contribution identifier	(5b1)	
Measurement equation parameter(s) subject to effect	Differential slant column of ozone	
Contribution subject to effect (final product or sub-tree intermediate product)	Quality controlled total column O_3 VCD	
Time correlation extent & form	Systematic	
Other (non-time) correlation extent & form	None	
Uncertainty PDF shape	Normal	
Uncertainty & units (1σ)	±0 nm	Unquantified
Sensitivity coefficient	1	
Correlation(s) between affected parameters	The same calibration is used for the noon reference spectrum and the twilight spectra	
Element/step common for all sites/users?	Yes	
Traceable to …	Community agreed procedure	Wavelength calibration procedure is available at http://uv-vis.aeronomie.be/software/QDOAS/QDOAS_manual.pdf
Validation	N/A since specific for each instrument	

6.11 **Laboratory absorption cross-sections (5b2)**

Comparison studies (e.g. Orphal, 2003) showed that differences of up to 4% in the ozone values depending on the cross-section sources can occur in the region of the Chappuis bands, and even more in the Huggins bands. Therefore the recommendation is the use of a common ozone cross-section data set to avoid systematic differences (Hendrick et al. 2011). From test evaluations, the O_3 cross-section of Bogumil et al. (2003) is recommended since it gives the smallest variance in the residuals as well as good consistency with the ozone retrieval in the UV Huggins bands. Vandaele et al. (1997) at 220 K is generally used for stratospheric NO_2 retrievals and therefore adequate for NO_2 removal in the O_3 fitting range (Hendrick et al., 2011).

Information / data	Type / value / equation	Notes / description
Name of effect	Laboratory absorption cross-sections	O_3 - Bogumil et al. (2003), 223K NO_2 - Vandaele et al. (1997), 220K H_2O - Hitran 2010 (Rothman et al., 2010)

		O4 - Hermans (http://spectrolab.aeronomie.be/o2.htm)
Contribution identifier	(5b2)	
Measurement equation parameter(s) subject to effect	Differential slant column of ozone	
Contribution subject to effect (final product or sub-tree intermediate product)	Quality controlled total column O_3 VCD	
Time correlation extent & form	Systematic – across data set in VO	
Other (non-time) correlation extent & form	None	
Uncertainty PDF shape	Normal	
Uncertainty & units (1σ)	Units are cm^2/molec. O_3 XS specifically introduces an uncertainty of 3% (systematic)	The uncertainty on the O_3 XS is the main contributor compared to the other species (NO_2, H_2O, etc.)
Sensitivity coefficient	1	O_3 uncertainties due to the indirect impact of uncertainties on other cross-section are related to cross-correlation effects. Largest interferences are due to water vapour and O_4 absorption bands which occasionally can lead to significant interference with ozone. On extreme cases (very humid or heavy cloud contamination), errors of several percent can occur. To minimise the impact of such effects, spectra contaminated by strong H_2O or O_4 absorptions are flagged or excluded from the retrieval.
Correlation(s) between affected parameters	Possible	Yes, there can be correlations between the overlapping XSs, hence wavelengths intervals are carefully chosen to minimize that effect.
Element/step common for all sites/users?	Yes	
Traceable to …	Cross-sections databases (e.g. HITRAN).	
Validation	Cross-sections comparison exercises.	

6.12 Ring effect cross-sections (5b3)

In short: For the correction of the Ring effect "filling-in" solar Fraunhofer lines, the approach published in Chance and Spurr (1997) is still recommended. The ozone differential absorption features are broad enough in the Chappuis bands to ensure that their filling-in by the Ring effect is quite small. However, due to its impact on the Fraunhofer lines, the Ring effect cannot be neglected and is usually treated as a "pseudo" absorber.

More detailed background: Because of Rotational Raman Scattering (RRS), a small fraction of the incident photons undergo a wavelength change of a few nanometres, i.e. a part of the scattering is inelastic. This causes an intensity loss at their incident wavelength and a gain at the neighbouring wavelengths to which they are redistributed. RRS causes the so-called "filling-in" of Fraunhofer lines, which have a slightly different shape in the "earthshine" radiance than in the direct solar light. This effect was first discovered by Grainger and Ring (ref) and is referred to as the Ring effect.

The atmospheric absorption lines are also broadened by RRS events occurring after absorption (molecular Ring effect). Although RRS accounts for only a few percent of the measured intensity, it significantly affects DOAS measurements of scattered radiation since typical trace gas absorptions are of the order of a percent or less. If not properly corrected, the Ring effect can produce strongly structured residuals in the differential optical density, due to the fact that Fraunhofer lines do not cancel perfectly between I and I_o.

Usually the Ring effect is taken into account by including an additional absorber in the DOAS fit. Ring cross sections S_{Ring} can be measured (Solomon et al., 1987) or calculated (Chance and Spurr, 1997). The Ring effect can then be approximated using the following development for an optically thin atmosphere (Van Roozendael et al., 2002; Wagner, 1999) and the QDOAS tool calculates a Ring cross-section according to the approach discussed in Wagner, 1999. The Ring effect is generally a major contributor to the differential absorption spectrum, since rotational Raman scattered light typically represents a few percent of the total scattered light. It is therefore critical to include a correction for the Ring effect. Neglecting this effects leads to substantial systematic residual features that may bias ozone DSCDs by several percent due to cross-correlation effect.

Information / data	Type / value / equation	Notes / description
Name of effect	Ring effect cross-sections	http://uv-vis.aeronomie.be/software/QDOAS/QDOAS_manual.pdf
Contribution identifier	(5b3)	
Measurement equation parameter(s) subject to effect	Differential slant column of ozone	
Contribution subject to effect (final product or sub-tree intermediate product)	Quality controlled total column O_3 VCD	
Time correlation extent & form	Method uncertainties are systematic	

Other (non-time) correlation extent & form	None	
Uncertainty PDF shape	Normal	
Uncertainty & units (1σ)	Units are cm^2/molec. As the other cross-sections	This Ring cross-section is fitted together with all other absorption cross-sections, and the resulting uncertainty in that fit is included the general uncertainty of the DOAS fit.
Sensitivity coefficient	1	
Correlation(s) between affected parameters	None	
Element/step common for all sites/users?	Yes	
Traceable to …	Community agreed procedure	
Validation	Informal exercises within intercomparison campaigns	e.g. Piters et al., 2012; Roscoe et al, 2010, Vandaele et al., 2005

6.13 Differential Slant Column Densities (DSCDs) (6)

Molecular absorption cross-sections are fitted to the logarithm of the ratio spectrum (5) – the ratio of the measured spectrum and the reference spectrum (i.e. a spectrum measured around local noon when the light path is at a minimum for ground-based measurements). The resulting fit coefficients are the integrated number of molecules per unit area along the atmospheric light path for each trace gas, the **differential slant column densities (SCDs)** which are the direct product of the DOAS analysis.

Information / data	Type / value / equation	Notes / description
Name of effect	Differential Slant Column Densities (DSCDs)	This is not a processing step but describes an important interim product in the processing chain including uncertainties Hendrick et al. (2011)
Contribution identifier	(6)	
Measurement equation parameter(s) subject to effect	DSCD, RCD	
Contribution subject to effect (final product or sub-tree	Quality controlled total column O_3 VCD	

intermediate product)		
Time correlation extent & form	Systematic	
Other (non-time) correlation extent & form	None	
Uncertainty PDF shape	normal	
Uncertainty & units (1σ)	13.45×10^{19}; Uncertainty in molec./cm^2 In general, 3% uncertainty in the ozone DSCDs	
Sensitivity coefficient	1	
Correlation(s) between affected parameters	None	
Element/step common for all sites/users?	Yes	
Traceable to …	Community agreed procedure	
Validation	Intercomparison campaigns	e.g. Piters et al., 2012; Roscoe et al, 2010, Vandaele et al., 2005

6.14 **Residual amount in reference spectrum – Langley plot approach (7)**

The amount of O_3 present in the optical light path to the instrument minus the amount present in a reference measurement (RCD), is the direct product of the DOAS analysis (see Sect. 4). The RCD is derived using the so-called **Langley plot method**, which consists in rearranging Eq. (1) in Sect. 4 and plotting DSCD(Θ) as a function of AMF(Θ), the intercept at AMF=0 giving the RCD (Roscoe et al., 1994; Vaughan et al., 1997).

Information / data	Type / value / equation	Notes / description
Name of effect	Langley plot approach	To determine the residual amount in the reference spectrum (RCD) using the Langley plot approach. Van Roozendael et al. (1998), Also: https://en.wikipedia.org/wiki/Langley_extrapolation
Contribution identifier	(7)	
Measurement equation parameter(s) subject to effect	Absolute SCD: DSCD+RCD	

Contribution subject to effect (final product or sub-tree intermediate product)	Quality controlled total column O_3 VCD	
Time correlation extent & form	Systematic over reference spectrum measurement cycle.	At Harestua and Jungfraujoch, the DOAS analysis is done using daily noon reference spectra, so the Langley plot approach is applied on a daily basis.
Other (non-time) correlation extent & form	Langley plot can only be done on clear mornings or evenings so have a synoptic correlation.	
Uncertainty PDF shape	Normal	
Uncertainty & units (1σ)	~3%; absolute numbers expressed in molec./cm^2 Approx. 2% of the total error budget.	
Sensitivity coefficient	1	
Correlation(s) between affected parameters	No	
Element/step common for all sites/users?	Yes	
Traceable to …	Community agreed procedure and standard	
Validation	Intercomparison campaigns	Informal validation

6.15 **Extracted AMFs (7a)**

So far, NDACC UV-visible groups commonly use their own DOAS settings and ozone AMFs calculated with different RTMs and sets of ozone, pressure and temperature profiles, with or without latitudinal and seasonal variations. Differences between AMFs are causing the largest discrepancies between the NDACC ozone data sets. The NDACC UV-visible WG provides recommendations to reduce these discrepancies through the use of standardized DOAS settings and O_3 AMF look-up tables (LUTs) calculated using the TOMS version 8 (TV8) O_3 profile climatology that account for the latitudinal and seasonal dependencies of the O_3 vertical profile (Hendrick et al., 2011; see also Sect. 4).
AMFs are extracted for any given station using an interpolation routine in Fortran fed by the LUTs and input values for location (latitude, longitude, altitude) of the station, time of the measurements, wavelength, surface albedo, solar zenith angle (SZA; θ in the table below) .

Information / data	Type / value / equation	Notes / description
Name of effect	Extracted AMFs	Ozone AMFs extracted for time, location and surface albedo
Contribution identifier	(7a)	
Measurement equation parameter(s) subject to effect	RCD, VCD	
Contribution subject to effect (final product or sub-tree intermediate product)	Quality-controlled total column O_3 VCD	
Time correlation extent & form	Systematic – given site methodology	
Other (non-time) correlation extent & form	None	
Uncertainty PDF shape	Normal	
Uncertainty & units (1σ)	mean uncertainty on AMF: 3.6% (1σ); no unit. 3.6% corresponds to 3.2e17 molec/cm^2 (12 Dobson unit) for a VCD value of 8.9e18 molec/cm^2 (330 Dobson Unit), which is a typical yearly mean value for O_3 VCD at 90°SZA at Harestua. Similar values are found at Jungfraujoch where the yearly mean O_3 VCD at 90°SZA is about 8.3e18 molec/cm^2 (310 Dobson Unit)	Derived by adding in quadrature the uncertainties related to the choice of the O_3 profile climatology, clouds, aerosols, albedo, and choice of the radiative transfer model for calculating AMFs.
Sensitivity coefficient	1	
Correlation(s) between affected parameters	None	
Element/step common for all sites/users?	LUTs and extraction routine are common for all stations.	
Traceable to ...	Community approved procedure	Hendrick et al. (2011)
Validation	AMF LUTs have been validated by comparison to AMFs calculated from O_3 sonde and lidar profiles at a selection of stations.	Hendrick et al. (2011)

6.16 **AMF, AVK, ozone profile, and effective airmass location extraction (7a1)**

The AMF is a key element in the VCD retrieval and its extraction is described in 6.15. AVK, ozone

profile, and effective air mass location are provided as ancillary information in the final GEOMS HDF files but are not part of the VCD retrieval itself (ozone profiles are indirectly involved in the retrieval since they are used to generate AMF LUT; see Sect. 6.15). They are all extracted from ad-hoc LUTs (see Hendrick et al., 2011; http://nors.aeronomie.be/projectdir/PDF/D4.4_NORS_SR.pdf). Effective air mass location (expressed in latitude, longitude) are derived using a LUT of horizontal displacement depending on the SZA and altitude. The interpolated horizontal displacement vertical profile is then converted into a latitude, longitude profile based on the solar azimuth angle at the measurement time.

Information / data	Type / value / equation	Notes / description
Name of effect	AMF, AVK, ozone profile, effective airmass location extraction	
Contribution identifier	(7a1)	
Measurement equation parameter(s) subject to effect	RCD and AMF	In contrast to AMF (see 7a), AVK, ozone profiles, and air mass location do not affect any measurement equation parameter.
Contribution subject to effect (final product or sub-tree intermediate product)	Quality controlled total ozone VCDs for AMF	AVK, ozone profiles, and effective air mass location are used to characterize the retrieved O_3 VCD but are not part of its retrieval. Ancillary data only & not effecting the measurement equation parameters
Time correlation extent & form	Systematic - presumably over full dataset time period.	
Other (non-time) correlation extent & form	None	
Uncertainty PDF shape	Normal	
Uncertainty & units (1σ)	0 (no units)	The uncertainties of these ancillary datasets are not included since they are not part of the data retrieval – purely there as additional information if found helpful for the interpretation of the results
Sensitivity coefficient	1	
Correlation(s) between affected parameters	N/A	
Element/step common for all	Yes, within the BIRA sites	Other site operators have different protocols.

sites/users?		
Traceable to …	Community approved procedure	Hendrick et al. (2011) for AMF, AVK, and ozone profiles; for effective air mass location, see http://nors.aeronomie.be/projectdir/PDF/D4.4_NORS_SR.pdf
Validation	AMF LUTs have been validated through comparison to AMFs calculated from O_3 sonde and lidar profiles at a selection of 9 stations (Hendrick et al., 2011). O_3 profiles from the TOMS version 8 have been validated through comparison to O_3 sonde profiles at about 40 stations located all around the world (McPeters et al., 2007). AVK and effective air mass location have not been validated so far.	

6.17 Latitude & longitude of the instrument (7a2)

Latitude and longitude of the instrument are used to extract AMF and ancillary parameters (AVK, effective air mass location). They are taken from the list of NDACC stations (http://www.ndsc.ncep.noaa.gov/sites/).

Information / data	Type / value / equation	Notes / description
Name of effect	Latitude and longitude of the instrument	
Contribution identifier	(7a2)	
Measurement equation parameter(s) subject to effect	AMF and RCD calculations	AVK and effective air mass location are ancillary parameters only and do not affect measurement equation parameters.
Contribution subject to effect (final product or sub-tree intermediate product)	Quality controlled total column O_3 VCD	
Time correlation extent & form	Systematic – list updates.	
Other (non-time) correlation extent & form	None	
Uncertainty PDF shape	Normal	

Uncertainty & units (1σ)	Uncertainty is in 0°.	The uncertainty on the position of the instruments has not been estimated so far. Sensitivity tests show that a difference of 0.1° on the latitude or longitude of the instrument has an impact of less than 0.02% on the AMF, and therefore on the RCD determination.
Sensitivity coefficient	Not estimated.	
Correlation(s) between affected parameters	SZA, AMF	
Element/step common for all sites/users?	Yes	
Traceable to …	Location logged with GPS	http://www.ndsc.ncep.noaa.gov/sites/
Validation	No validation of the latitude and longitude of the instrument done so far.	

6.18 **Altitude of station (7a3)**

The altitude of an instrument is used to extract AMF and ancillary parameters (AVK, effective air mass location). It is taken from the list of NDACC stations (http://www.ndsc.ncep.noaa.gov/sites/).

Information / data	Type / value / equation	Notes / description
Name of effect	Altitude	Altitude of the instrument
Contribution identifier	(7a3)	
Measurement equation parameter(s) subject to effect	AMF and RCD	
Contribution subject to effect (final product or sub-tree intermediate product)	Quality controlled total column O_3 VCD	
Time correlation extent & form	Systematic over dataset time period.	
Other (non-time) correlation extent & form	None	
Uncertainty PDF shape	Normal	
Uncertainty & units (1σ)	A few meters.	Looking at the NDACC AMF LUTs, the impact on AMF of

		taking a site altitude of 4km instead of 0km is 5%. Therefore, an uncertainty of a few meters on the altitude of the station has a negligible impact on the AMF and on the VCD.
Sensitivity coefficient	1	
Correlation(s) between affected parameters	None	
Element/step common for all sites/users?	Yes	
Traceable to …	Altitude logged with GPS	http://www.ndsc.ncep.noaa.gov/sites/
Validation	No validation of the altitude of the instrument is done.	

6.19 AMF & AVK look-up tables, horizontal displacement & TOMS climatology (7a4)

O_3 AMFs and AVK are extracted from LUTs calculated using the TOMS version 8 (TV8) O_3 profile climatology, from which the O_3 vertical profiles reported in the GEOMS files are also extracted. The horizontal displacement LUT has been created by simple ray tracing calculation using the standard AFGL 1976 atmosphere (http://nors.aeronomie.be/projectdir/PDF/D4.4_NORS_SR.pdf). Only the AMFs are used in the retrieval of O_3 VCDs, the other parameters being provided as ancillary information in the GEOMS HDF files.

Information / data	Type / value / equation	Notes / description
Name of effect	AMF and AVK LUTs, horizontal displacement LUT, TOMS V8 ozone profile climatology	See table (6.16)
Contribution identifier	(7a4)	
Measurement equation parameter(s) subject to effect	AMF LUTs and TOMS version 8 climatology affect AMF and RCD	AVK and horizontal displacement (effective air mass location) are ancillary parameters only and do not affect measurement equation parameters.
Contribution subject to effect (final product or sub-tree intermediate product)	Quality controlled total column O_3 VCD	
Time correlation extent & form	Systematic	
Other (non-time)	Assumed 1976 profiles –	

correlation extent & form	presumably changed since.	
Uncertainty PDF shape	Normal	
Uncertainty & units (1σ)	AMF is unitless. – contributes to 3.6% on the O_3 VCD total uncertainty, which corresponds to 3.2e17 molec/cm^2 (12 Dobson Unit) for a VCD value of 8.9e18 molec/cm^2 (330 Dobson Unit), which is a typical yearly mean value for O_3 VCD at 90°SZA at Harestua. Similar values are found at Jungfraujoch where the yearly mean O_3 VCD at 90°SZA is about 8.3e18 molec/cm^2 (310 Dobson Unit)	See table 6.16
Sensitivity coefficient	1	
Correlation(s) between affected parameters	None	
Element/step common for all sites/users?	Yes	
Traceable to …	Hendrick et al. (2011) for AMF and AVK; McPeters et al. (2007) for TOMS version 8 climatology, and http://nors.aeronomie.be/projectdir/PDF/D4.4_NORS_SR.pdf for effective air mass location.	
Validation	AMF LUTs have been validated through comparison to AMFs calculated from O_3 sonde and lidar profiles at a selection of 9 stations (Hendrick et al., 2011). O_3 profiles from the TOMS version 8 climatology have been validated through comparison to O_3 sonde profiles at about 40 stations located all around the world (McPeters et al., 2007). AVK and effective air mass location have not been validated so far.	

6.20 **Decimal day number (7a5)**

The decimal day number corresponding to each measurement is determined using the computer clock. Since the latter is generally updated online to a time server (e.g. NTP), the uncertainty introduced this way should be minimal.

Information / data	Type / value / equation	Notes / description
Name of effect	Decimal day number	
Contribution identifier	(7a5)	
Measurement equation parameter(s) subject to effect	AMF calculation	
Contribution subject to effect (final product or sub-tree intermediate product)	Quality controlled total column O_3 VCD	
Time correlation extent & form	Computers controlling the instruments are synchronised in time once per day with server like NTP.	
Other (non-time) correlation extent & form	None	
Uncertainty PDF shape	Normal	
Uncertainty & units (1σ)	Assumed negligible compared to other contributions	
Sensitivity coefficient	1	
Correlation(s) between affected parameters	SZA	The deviation of the computer clock with respect to the time server over 24h is about 5s at maximum. Therefore the impact on the SZA is expected to be small, even at high SZA.
Element/step common for all sites/users?	Yes	
Traceable to ...	N/A	
Validation	Validation of the internal clock to time server like NTP.	

6.21 Solar Zenith Angle (SZA) (7a6)

As knowledge of the solar zenith angle (SZA) is crucial for the computation of air mass factors, in particular for stratospheric applications, accurate time has to be saved with the observations. The exact time is usually provided by a GPS sensor or – in case of separated instruments situated indoors – via network time synchronisation. The Solar Zenith Angle (SZA) is directly calculated from the time stamp of the measured raw spectrum, generally using the Meeus (1998) algorithm.

Information / data	Type / value / equation	Notes / description
Name of effect	Solar Zenith Angle (SZA)	
Contribution identifier	(7a6)	
Measurement equation parameter(s) subject to effect	AMF and RCD dependent on the SZA	
Contribution subject to effect (final product or sub-tree intermediate product)	Quality controlled total column O_3 VCD	
Time correlation extent & form	Systematic	
Other (non-time) correlation extent & form	None	
Uncertainty PDF shape	Normal	
Uncertainty & units (1σ)	0.01 in degree	Assumed, to be confirmed by sensitivity study
Sensitivity coefficient	cos(SZA)	True until high SZA (to be determined)
Correlation(s) between affected parameters	time (7a5)	
Element/step common for all sites/users?	Yes	For sites other than those on VO, uncertainty can be different
Traceable to …	Meeus, J. "Astronomical Algorithms". Second edition 1998, Willmann-Bell, Inc.,Richmond, Virginia, USA	
Validation	Through intercomparison campaign such as CINDI & CINDI-2	Piters et al., 2012; Roscoe et al, 2010, Vandaele et al., 2005

6.22 Surface albedo climatology (7a7)

A global monthly mean climatology of the surface albedo derived from satellite data at 494 nm (Koelemeijer et al., 2003) is coupled to the interpolation routine, so the latter can be initialized

with realistic albedo values in a transparent way (Hendrick et al., 2011). The interpolation routine, O_3 AMF LUTs, albedo climatology as well as DOAS settings are publicly available at http://uv-vis.aeronomie.be/groundbased.

Information / data	Type / value / equation	Notes / description
Name of effect	Surface albedo climatology	
Contribution identifier	(7a7)	
Measurement equation parameter(s) subject to effect	AMF; AVK depends also on surface albedo but it does not play any role (only ancillary information) in the O_3 VCD retrieval	
Contribution subject to effect (final product or sub-tree intermediate product)	Quality controlled total column O_3 VCD	
Time correlation extent & form	None	
Other (non-time) correlation extent & form	None	
Uncertainty PDF shape	Normal	
Uncertainty & units (1σ)	~0.02 at 335nm; Albedo has no units Assumed negligible	Koelemeijer et al. (2003) Note: the topography is taken into account in the climatology through the use of a surface pressure database
Sensitivity coefficient	Not determined but given the zenith viewing geometry, the impact of albedo on AMF is very small (<0.7% when going from an albedo value of 0.04 (ice free sea) to 1 (fresh snow); see Hendrick et al., 2011).	
Correlation(s) between affected parameters	None	
Element/step common for all sites/users?	Yes	
Traceable to ...	Koelemeijer et al. (2003)	
Validation	Comparison of Koelemeijer et al. (2003) surface albedo database to TOMS measurements showed satisfactory agreement.	

6.23 Absolute slant column densities (SCDs) (8)

The obtention of absolute slant column densities (SCDs) is the end product of the first step of the O_3 VCD retrieval (the second step being the conversion of these SCDs into VCDs using the AMFs).

Information / data	Type / value / equation	Notes / description
Name of effect	Quality controlled SCDs	
Contribution identifier	(8)	
Measurement equation parameter(s) subject to effect	VCD	
Contribution subject to effect (final product or sub-tree intermediate product)	Quality controlled total column O_3 VCD	
Time correlation extent & form	Systematic	
Other (non-time) correlation extent & form	None	
Uncertainty PDF shape	Normal	
Uncertainty & units (1σ)	Overall uncertainty of ~5%; , which corresponds to 7.5e18 molec/cm^2 for an absolute SCD value of 1.5e20 molec/cm^2, which is a typical yearly mean value for O_3 SCD at 90°SZA at Harestua. Similar values are found at Jungfraujoch where the yearly mean O_3 SCD at 90°SZA is about 1.4e18 molec/cm^2	
Sensitivity coefficient	1	
Correlation(s) between affected parameters	None	
Element/step common for all sites/users?	Yes	
Traceable to …	Community approved process	e.g. Hendrick et al. (2011)
Validation	N/A	

6.24 Conversion of SCDs into vertical column densities (VCDs) (9)

The conversion of SCDs into vertical column densities (VCDs) is the second and last step of the O_3 VCD retrieval. It consists in dividing the SCDs by appropriate AMFs to get VCDs.

Information / data	Type / value / equation	Notes / description
Name of effect	Conversion of SCDs into VCDs	
Contribution identifier	(9)	
Measurement equation parameter(s) subject to effect	$VCD(\theta) = \frac{SCD(\theta)}{AMF(\theta)}$	
Contribution subject to effect (final product or sub-tree intermediate product)	Quality controlled total column O_3 VCD	
Time correlation extent & form	Systematic – a linearised assumption?	
Other (non-time) correlation extent & form	None	
Uncertainty PDF shape	N/A	
Uncertainty & units (1σ)	N/A	
Sensitivity coefficient	1	
Correlation(s) between affected parameters	N/A	
Element/step common for all sites/users?	Yes	
Traceable to …	N/A	
Validation	N/A	

6.25 **VCDs quality screening (10)**

Each group has its own quality screening procedure for VCDs. In the case of the BIRA spectrometers at Harestua and Jungfraujoch, it is done through the removal of data with large fit residuals and the visual inspection of the O_3 VCD time-series (plots of VCDs versus time and comparison between neighbourhood data point values).

Information / data	Type / value / equation	Notes / description
Name of effect	VCDs quality screening	
Contribution identifier	(10)	
Measurement equation parameter(s) subject to effect	VCD' = VCD	
Contribution subject to effect (final product or sub-tree intermediate product)	Quality controlled total column O_3 VCD	
Time correlation extent & form	Systematic	

Other (non-time) correlation extent & form	N/A	
Uncertainty PDF shape	Screening process can change the overall distribution of the uncertainty since the number of higher uncertainty will decrease after the screening.	
Uncertainty & units (1σ)	N/A	
Sensitivity coefficient	1	
Correlation(s) between affected parameters	No	
Element/step common for all sites/users?	No; each group has its own quality screening criteria.	
Traceable to …	N/A	
Validation	N/A	

6.26 Quality controlled total O_3 VCDs (11)

Quality controlled total O_3 VCDs are the end product resulting from the VCDs quality screening.

Information / data	Type / value / equation	Notes / description
Name of effect	Quality controlled	Hendrick et al. (2011)
Contribution identifier	(11)	
Measurement equation parameter(s) subject to effect	N/A	
Contribution subject to effect (final product or sub-tree intermediate product)	Quality controlled total column O_3 VCD	
Time correlation extent & form	None	
Other (non-time) correlation extent & form	None	
Uncertainty PDF shape	Normal	
Uncertainty & units (1σ)	Overall uncertainty of ~6%; , which corresponds to 5.3e17 molec/cm^2 (19.8 Dobson Unit) for a VCD value of 8.9e18 molec/cm^2 (330 Dobson Unit), which is a typical yearly mean	

	value for O_3 VCD at 90°SZA at Harestua. Similar values are found at Jungfraujoch where the yearly mean O_3 VCD at 90°SZA is about 8.3e18 molec/cm^2 (310 Dobson Unit)	
Sensitivity coefficient	1	
Correlation(s) between affected parameters	N/A	
Element/step common for all sites/users?	Yes	
Traceable to …	N/A	
Validation	Intercomparison campaigns.	e.g. Piters et al., 2012; Roscoe et al, 2010, Vandaele et al., 2005

6.27 GEOMS HDF creation routine (12)

O_3 VCDs and ancillary information (AVKs, O_3 vertical profiles, and effective air mass location) are converted from their native ascii format to the GEOMS HDF4 format using the GEOMS UVVIS DOAS templates and conversion routines available at https://avdc.gsfc.nasa.gov/index.php?site=1876901039.

There is no new uncertainty in this process.

Information / data	Type / value / equation	Notes / description
Name of effect	GEOMS HDF creation routine	https://avdc.gsfc.nasa.gov/index.php?site=1876901039
Contribution identifier	(12)	
Measurement equation parameter(s) subject to effect	N/A	
Contribution subject to effect (final product or sub-tree intermediate product)	Quality controlled total column O_3 VCD	
Time correlation extent & form	None	
Other (non-time) correlation extent & form	None	
Uncertainty PDF shape	N/A	
Uncertainty & units	N/A	

(1σ)		
Sensitivity coefficient	N/A	
Correlation(s) between affected parameters	N/A	
Element/step common for all sites/users?	Yes, except that data providers can also use their own ASCII to GEOMS conversion routines.	
Traceable to …	N?A	
Validation	No validation required; GEOMS HDf files can be tested again the GEOMS QA/QC checker available at https://avdc.gsfc.nasa.gov/index.php?site=1829327959.	

6.28 Extracted AVKs, ozone profiles, and effective airmass location (12a)

Extracted AVKs, ozone profiles and effective air mass location are provided as ancillary information to the O_3 VCDs reported in the GEOMS HDF files. They do not affect any measurement equation parameter and are a specific subset of (7a1).

Information / data	Type / value / equation	Notes / description
Name of effect	Extracted AVKs, ozone profiles, and effective airmass location	
Contribution identifier	(12a)	
Measurement equation parameter(s) subject to effect	Extracted AVKs, ozone profiles, and effective airmass location are provided as ancillary information and do not affect any measurement equation parameter.	
Contribution subject to effect (final product or sub-tree intermediate product)	Quality controlled total column O_3 VCD	
Time correlation extent & form	None	
Other (non-time) correlation extent & form	None	
Uncertainty PDF shape	Normal	
Uncertainty & units (1σ)	N/A	
Sensitivity coefficient	1	

Correlation(s) between affected parameters	N/A	
Element/step common for all sites/users?	Yes	
Traceable to …	http://ndacc-uvvis-wg.aeronomie.be/tools.php	
Validation	O_3 profiles extracted from the TOMS version 8 climatology have been validated through comparison to O_3 sonde profiles at about 40 stations located all around the world (McPeters et al., 2007). AVK and effective air mass location have not been validated so far.	

6.29 GEOMS UV-vis total O_3 data file (13)

The GEOMS UV-vis total O_3 file is the total O_3 column retrieval end product which is made available to users.

Information / data	Type / value / equation	Notes / description
Name of effect	GEOMS UV-vis total O_3 data file	This is the final product
Contribution identifier	(13)	
Measurement equation parameter(s) subject to effect	N/A	
Contribution subject to effect (final product or sub-tree intermediate product)	N/A	
Time correlation extent & form	None	
Other (non-time) correlation extent & form	None	
Uncertainty PDF shape	N/A	
Uncertainty &	N/A	

units (1σ)		
Sensitivity coefficient	N/A	
Correlation(s) between affected parameters	N/A	
Element/step common for all sites/users?	Yes	
Traceable to …	NDACC database (http://www.ndacc.org)	
Validation	No validation required; GEOMS HDF files can be tested again the GEOMS QA/QC checker available at https://avdc.gsfc.nasa.gov/index.php?site=1829327959 .	

7 Uncertainty Summary

Element identifier	Contribution name	Uncertainty contribution form	Typical value	Traceability level (L/M/H)	random, structured random, quasi-systematic or systematic?	Correlated to? (Use element identifier)
1	Raw radiance spectra	L_{raw}noise = √signal (Photon noise in counts)	0.01-0.1% (negligible compared to other uncertainties)	N/A	random	4
2	Offset and dark signal correction	DarkNoise= √DarkSignal	Around 0.1%	M	random & systematic	none
3	Wavelength calibration	wavelength shift & stretch	<0.1 nm	H	systematic	none
3a	High resolution solar Fraunhofer atlas	wavelength accuracy	3.5-4%	H	systematic	none
3b	Instrument slit function	shape of slit function	<0.1%	M	random	none
4	Wavelength calibrated radiance spectra	wavelength accuracy	<0.1nm, based on (3)	M	random & systematic	1
5	DOAS spectral fit	fitting uncertainty	$13.45x10^{19}$ molec./cm^2	M	random & systematic	none
5a	Retrieval strategy	N/A	N/A	N/A	N/A	N/A
5b	Cross-sections at instrument resolution	XS shape & wavelength calibration	<0.1%	M	random & systematic	5b2
5b1	Calibrated wavelength grid	wavelength accuracy	<0.1 nm	M	random & systematic	3,4
5b2	Laboratory absorption cross-section	XS shape & wavelength calibration	3% for ozone	M	random & systematic	5b
5b3	Ring effect cross-sections	Ring XS calculations	estimated roughly 5%	L	random & systematic	none
6	Differential Slant Column Densities (DSCDs)	Combined uncertainty in DSCDs	$13.45x10^{19}$ molec./cm^2 or 3%	M	random & systematic	none
7	Residual amount in reference spectrum – Langley plot approach	Langley extra-polation	~3%	M	random & systematic	7a

7a	Extracted AMFs	Differences in AMF calculation approaches	3.6% mean uncertainty	M	random	7a1, 7a4, 12a
7a1	AMF, AVK, ozone profile, and effective airmass location extraction	not effecting the data product uncertainty	N/A	N/A	N/A	7a
7a2	Latitude & longitude of the instrument	exact location	assumed negligible	M	random	none
7a3	Altitude of station	exact altitude	assumed negligible	M	random	none
7a4	AMF & AVK look-up tables, horizontal displacement & TOMS climatology	TOMS climatology	3.6% on O_3 VCD	M	random & systematic	7a
7a5	Decimal day number	accuracy of date & time	assumed negligible	H	random	7a6
7a6	Solar Zenith Angle (SZA)	accuracy of time	0.01°	H	random	7a5
7a7	Surface albedo climatology	accuracy of surface albedo values	assumed negligible	M	random	none
8	Quality controlled absolute slant column densities (SCDs)	combined uncertainty in calculated SCDs	~5%	M	random & systematic	6, 11
9	Conversion of SCDs into vertical column densities (VCDs)	N/A	N/A	N/A	N/A	N/A
10	VCDs quality screening	N/A	N/A	N/A	N/A	N/A
11	Quality controlled total O_3 VCDs	combined uncertainty in calculated VCDs	~6% corresponds to $5.3e^{17}$ molec./cm^2 or 19.8 DU	H	random & systematic	8
12	GEOMS HDF creation routine	N/A	N/A	N/A	N/A	N/A
12a	Extracted AVKs, ozone profiles, and effective	N/A	N/A	N/A	N/A	N/A

	airmass location					
13	GEOMS UV-vis total O_3 data file	Same as (11)	~6%	H	Systematic + random	11

The element components of the main chain are shown in bold.

Table 2 shows the uncertainty budget from Hendrick et al. 2011, that, although it contains a different set of contributions, results in a similar overall uncertainty estimate of 6% (1σ). The uncertainty contributions are assumed independent & randomly distributed, so combined in quadrature.

Table 2. Uncertainty summary table from Hendrick et al 2011, table 4 with the corresponding element contribution numbers alongside. Items with an asterisk indicate this is part of an element contribution in this PTU document.

Table 4. Error budget of zenith-sky total O_3 columns measurements in the visible (%).

Error source	Error (%)	
(a) Random		
Slant column spectral fit, including interference effects	3	(7)
O_3 AMF		
TV8 climatology	1.0	(7a4)*
Clouds	3.3	(7a4)*
Aerosols	0.6	(7a4)*
Albedo	0.7	(7a7)
RTM	0.7	
Precision	**4.7**	
(b) Systematic		
O_3 cross sections	3.0	(5b2)
Residual column	2.0	(7)
Total Accuracy	**5.9**	(11 & 13)

8 Traceability uncertainty analysis

Traceability level definition is given in Table 3.

Table 3. Traceability level definition table

Traceability Level	Descriptor	Multiplier
High	SI traceable or globally recognised community standard	1
Medium	Developmental community standard or peer-reviewed uncertainty assessment	3
Low	Approximate estimation	10

Analysis of the summary table would suggest the following contributions, shown in Table 4, should be considered further to improve the overall uncertainty of the NDACC temperature product.

Table 4. Traceability level definition further action table.

Element identifier	Contribution name	Uncertainty contribution form	Typical value	Traceability level (L/M/H)	random, structured random, quasi-systematic or systematic?	Correlated to? (Use element identifier)
2	**Offset and dark signal correction**	**DarkNoise= √DarkSignal**	**Around 0.1%**	**M**	**random & systematic**	**none**
3b	Instrument slit function	**shape of slit function**	<0.1%	M	random	none
4	**Wavelength calibrated radiance spectra**	**wavelength accuracy**	**<0.1nm, based on (3)**	**M**	**random & systematic**	**1**
5	**DOAS spectral fit**	**fitting uncertainty**	**13.45×10^{19} molec./cm^2**	**M**	**random & systematic**	**none**
5b	Cross-sections at instrument resolution	XS shape & wavelength calibration	<0.1%	M	random & systematic	5b2
5b1	Calibrated wavelength grid	wavelength accuracy	<0.1 nm	M	random & systematic	3,4
5b2	Laboratory absorption cross-section	XS shape & wavelength calibration	3% for ozone	M	random & systematic	5b
5b3	Ring effect cross-sections	Ring XS calculations	estimated roughly 5%	L	random & systematic	none
6	**Differential Slant Column Densities (DSCDs)**	**Combined uncertainty in DSCDs**	**13.45×10^{19} molec./cm^2 or 3%**	**M**	**random & systematic**	**none**
7	**Residual amount in reference spectrum – Langley plot approach**	**Langley extra-polation**	**~3%**	**M**	**random & systematic**	**7a**
7a	Extracted AMFs	Differences in AMF calculation approaches	3.6% mean uncertainty	M	random	7a1, 7a4, 12a
7a2	Latitude & longitude of the instrument	exact location	assumed negligible	M	random	none
7a3	Altitude of station	exact altitude	assumed negligible	M	random	none
7a4	AMF & AVK look-up tables, horizontal displacement & TOMS	TOMS climatology	3.6% on O_3 VCD	M	random & systematic	7a

	climatology					
8	**Quality controlled absolute slant column densities (SCDs)**	**combined uncertainty in calculated SCDs**	**~5%**	**M**	**random & systematic**	**6, 11**

8.1 Recommendations

There are 15 contributions, see Table 4, that are not SI traceable or do not have a globally recognised community standard. Or, to be more precise, it is actually not so much that these contributions are not necessarily globally recognised or documented as part of reports but rather not as well represented in the peer-reviewed literature as prudent to acknowledge full traceability. One example is that differences in the exact method how to calculate AMFs still causes the largest discrepancies between different data sets. Further analysis and sensitivity studies to quantify and determine the magnitude of these potential contributions would better constrain the uncertainty budget and provide further confidence in traceability.

The contributions given in Table 4 can be divided into some general categories.

Contributions related to wavelength calibration (3, 4 & 5b1) although strictly not SI traceable, are referenced to line calibration lamps, a community standard across many spectroscopy disciplines. In as much, the additional (and onerous step) to SI traceability is unlikely to be necessary, and could be argued that is vicariously SI traceable through the literature wavelength values provided by NMIs such as NIST. The remaining issue for this product is a sensitivity assessment of the impact of the wavelength uncertainty on the retrieved product uncertainty.

Many contributions have ascribed uncertainty assessments in their native units, (cross-section uncertainty) that would not be independently verified by the product suppliers. As such, these uncertainties can be taken at face value. The remaining issue for this product is a sensitivity assessment of the impact of these uncertainty on the retrieved product uncertainty.

Contributions where no assessment of the element uncertainty (e.g. site location & altitude and time stamp uncertainty) has been undertaken, should be addressed. In many cases these are assumed negligible, however, some analysis to evidence this assumption would progress the uncertainty budget towards reference status.

The majority of contributions in Table 4 could be advanced towards reference status with sensitivity studies to understand how these uncertainties propagate to the retrieved product uncertainty.

The validation of the component uncertainty contributions could be made piece-wise, rather than in the cumulative uncertainty to add evidence to the assessment robustness.

9 Conclusion

The UV-visible total column ozone product has been assessed against the GAIA CLIM traceability and uncertainty criteria.

References

Bhartia, P. K., Wellemeyer, C. G., Taylor, S. L., Nath, N., and Gopolan, A., Solar Backscatter (SBUV) Version 8 profile algorithm, in: Proceedings of the Quadrennial Ozone Symposium 2004, Athens, Greece, edited by C. Zerefos, ISBN 960-630-103-6, pp. 295-296, 2004.

Bogumil, K., Orphal, J., Homann, T., Voigt, S., Spietz, P., Fleischmann, O. C., Vogel, A., Hartmann, M., Bovensmann, H., Frerik, J., and Burrows, J. P., Measurements of molecular absorption spectra with the SCIAMACHY Pre-Flight Model: Instrument characterization and reference spectra for atmospheric remote sensing in the 230-2380 nm region, J. Photochem. Photobiol. A, 157, 167–184, 2003.

Chance, K. and Spurr, R. J. D., Ring effect studies: Rayleigh scattering including molecular parameters for rotational Raman scattering, and the Fraunhofer spectrum, Applied Optics, 36, 5224-5230, 1997.

Chance, K. and Kurucz, R. L., An improved high-resolution solar reference spectrum for earth's atmosphere measurements in the ultraviolet, visible, and near infrared. Journal of Quantitative Spectroscopy and Radiative Transfer, 111(9):1289-1295, 2010.

Hendrick, F., Pommereau, J.-P., Goutail, F., Evans, R.D., Ionov, D., Pazmino, A., Kyrö, E., Held, G., Eriksen, P., Dorokhov, V., Gil, M., and Van Roozendael, M., NDACC/SAOZ UV-visible total ozone measurements: improved retrieval and comparison with correlative ground-based and satellite Observations, Atmos. Chem. Phys., 11, 5975–5995, doi:10.5194/acp-11-5975-2011, 2011.

Grainger, J. and Ring, J.: Anomalous Fraunhofer line profiles, Nature, 193, p. 762, 1962.

Koelemeijer, R. B. A., de Haan, J. F., and Stammes, P.: A database of spectral surface reflectivity in the range 335-772 nm derived from 5.5 years of GOME observations, J. Geophys. Res., 108(D2), 4070, doi:10.1029/2002JD002429, 2003.

McPeters, R. D., Labow, G. J., and Logan, J. A., Ozone climatological profiles for satellite retrieval algorithms, J. Geophys. Res., 112, D05308, doi:10.1029/2005JD006823, 2007.

NIST Atomic Spectra Database, https://physics.nist.gov/PhysRefData/ ASD/lines form. html [2018, January 15]. National Institute of Standards and Technology, Gaithersburg, MD.

Orphal, J.: A critical review of the absorption cross-sections of O_3 and NO_2 in the 240-790 nm region, J. of Photochem. and Photobiol. A: Chemistry, 157, 185-209, 2003.

Piters, A.J.M., Boersma, K.F., Kroon, M., Hains, J.C., Van Roozendael, M., Wittrock, F., Abuhassan, N., Adams, C., Akrami, M., Allaart, M.A.F., Apituley, A., Bergwerff, J.B., Berkhout, A.J.C., Brunner, D., Cede, A., Chong, J., Clémer, K., Fayt, C., Frieß, U., Gast, L.F.L., Gil-Ojeda, M., Goutail, F., Graves, R., Griesfeller, A., Großmann, K., Hemerijckx, G., Hendrick, F., Henzing, B., Herman, J., Hermans, C., Hoexum, M., van der Hoff, G.R., Irie, H., Johnston, P.V., Kanaya, Y., Kim, Y.J., Klein Baltink, H., Kreher, K., et al., The Cabauw Intercomparison campaign for Nitrogen Dioxide measuring Instruments (CINDI): design, execution, and early results, Atmospheric Measurement Techniques Discussions, 4, 5935-6005, 2012.

Platt, U. and Stutz, J.: Differential Optical Absorption Spectroscopy: Principles and Applications. Physics of Earth and Space Environments. Springer, Berlin, 2008.

Roscoe, H. K., Squires, J. A. C., Oldham, D. J., Sarkissian, A., Pommereau, J.-P., and Goutail, F.: Improvements to the accuracy of zenith-sky measurements of total ozone by visible spectrometers, J. Quant. Spectrosc. Radiat. Transfer, 52(5), 639-648, 1994.

Roscoe, H. K., Van Roozendael, M., Fayt, C., du Piesanie, A., Abuhassan, N., Adams, C., Akrami, M., Cede, A., Chong, J., Clémer, K., Friess, U., Gil Ojeda, M., Goutail, F., Graves, R., Griesfeller, A.,

Grossmann, K., Hemerijckx, G., Hendrick, F., Herman, J., Hermans, C., Irie, H., Johnston, P. V., Kanaya, Y., Kreher, K., Leigh, R., Merlaud, A., Mount, G. H., Navarro, M., Oetjen, H., Pazmino, A., Perez-Camacho, M., Peters, E., Pinardi, G., Puentedura, O., Richter, A., Schönhardt, A., Shaiganfar, R., Spinei, E., Strong, K., Takashima, H., Vlemmix, T., Vrekoussis, M., Wagner, T., Wittrock, F., Yela, M., Yilmaz, S., Boersma, F., Hains, J., Kroon, M., Piters, A., and Kim, Y. J.: Intercomparison of slant column measurements of NO_2 and O_4 by MAX-DOAS and zenith-sky UV and visible spectrometers, Atmos. Meas. Tech., 3, 1629–1646, doi:10.5194/amt-3-1629-2010, 2010.

Rothman, L. S., I.E. Gordon, R.J. Barber, H. Dothe, R.R. Gamache, A. Goldman, V.I. Perevalov, S.A. Tashkun, and J. Tennyson, HITEMP, the high-temperature molecular spectroscopic database, J. Quant. Spectroscopy Radiat. Transfer, 111, 2139-2150, 2010.

Solomon, S., Schmeltekopf, A. L., and Sanders, R. W., On the interpretation of zenith sky absorption measurements. Journal of Geophysical Research, 92(D7):8311-8319, 1987.

Vandaele, A. C., Hermans, C., Simon, P. C., Carleer, M., Colin, R., Fally, S., Mérienne, M.-F., Jenouvrier, A., and Coquart, B.: Measurements of the NO_2 absorption cross section from 42 000 cm−1 to 10 000 cm−1 (238–1000 nm) at 220 K and 294 K, J. Quant. Spectrosc. Ra., 59, 171–184, 1997.

Vandaele, A. C., Fayt, C., Hendrick, F., Hermans, C., Humbled, F., Van Roozendael, M., Gil, M., Navarro, M., Puentedura, O., Yela, M., Braathen, G., Stebel, K., Tørnkvist, K., Johnston, P., Kreher, K., Goutail, F., Mieville, A., Pommereau, J.-P., Khaikine, S., Richter, A., Oetjen, H., Wittrock, F., Bugarski, S., Frieß, U., Pfeilsticker, K., Sinreich, R., Wagner, T., Corlett, G., and Leigh, R.: An intercomparison campaign of ground-based UV-visible measurements of NO_2, BrO, and OClO slant columns: Methods of analysis and results for NO_2, J. Geophys. Res., 110, D08305, doi:10.1029/2004JD005423, 2005.

Van Roozendael, M., M. De Maziere, and P.C. Simon, Ground-based visible measurements at the Jungfraujoch station since 1990, J. Quant. Spectrosc. Radiat. Transfer, 52**,** 231–240, 1994.

Van Roozendael, M., Peters, P., Roscoe, H. K., De Backer, H., Jones, A. E., Bartlett, L., Vaughan, G., Goutail, F., Pommereau, J.-P., Kyrö, E., Wahlstrom, C., Braathen, G., and Simon, P. C., Validation of ground-based visible measurements of total ozone by comparison with Dobson and Brewer spectrophotometers, J. Atmos. Chem., 29, 55–83, 1998.

Van Roozendael, M., Soebijanta, V., Fayt, C., and Lambert, J., Investigation of DOAS issues affecting the accuracy of the GDP version 3.0 total ozone product. In ERS-2 GOME GDP 3.0 Implementation and Delta Validation, 2002.

Vaughan, G., Roscoe, H. K., Bartlett, L. M., O'Connor, F., Sarkissian, A., Van Roozendael, M., Lambert, J.-C., Simon, P. C., Karlsen, K., Kaestad Hoiskar, B. A., Fish, D. J., Jones, R. L., Freshwater, R., Pommereau, J.-P., Goutail, F., Andersen, S. B., Drew, D. G., Hughes, P. A., Moore, D., Mellqvist, J., Hegels, E., Klupfel, T., Erle, F., Pfeilsticker, K., and Platt, U.: An intercomparison of ground-based UV-visible sensors of ozone and NO_2, J. Geophys. Res., 102, 1411-1422, 1997.

Wagner, T., Satellite Observations of Atmospheric HalogenOxides. PhD thesis, University of Heidelberg, 1999.